新ナノテクノロジーを採用したコンポジット

レジン修復の新規生体光学技術による評価

OPTICAL COHERENCE TOMOGRAPHY IN DENTISTRY;

IMAGING, APPLICATIONS, SIGNAL ANALYSIS AND PROCESSING

The Role of Novel Biophotonic Technique in Characterization of the Newly Developed Nanotechnology-based Dental Composites

Doctoral of Philosophy Thesis

Turki A. Bakhsh

ターキ　バクシュ

A dissertation presented

by

Turki Abdulsalam A. BAKHSH

to

Cariology and Operative Dentistry,

Department of Oral Health Sciences,

Faculty of Dentistry,

Graduate School of Medical and Dental Sciences

in partial fulfillment of the requirements
for the degree of

Doctor of Philosophy

in Dental Science

Promoter: Prof. Junji TAGAMI
Advisers: Drs. Alireza SADR & Yasushi SHIMADA

Tokyo Medical and Dental University
Tokyo, Japan

September 2013

ABSTRACT

Promoter: Prof. Junji Tagami
Author: Dr. Turki Bakhsh
Cariology & Operative Dentistry

ABSTRACT

The Role of Novel Biophotonic Technique in Characterization of the Newly Developed Nanotechnology-based Dental Composites

[Background and Objective]: Polymerization shrinkage and the associated contraction stresses are the major shortcoming of dental composites in dentistry, which may affect the bonding performance and result in gap formation at the tooth-restoration interface. Non-destructive assessment and monitoring of these defects are critically important. The aim of this study is to assess the tooth-restoration interface and composite adaptation using swept source optical coherence tomography (SS-OCT) in combination of microtensile bond strength (MTBS) and to confirm the findings with confocal laser scanning microscope (CLSM) and scanning electron microscopy (SEM).

[Materials and Methods]: Standard round class-I cavities were prepared in human premolar teeth and restored according to the manufacturer instructions. The cavities were restored using different all-in-one adhesive system and composite restoration in different filling techniques. Serial cross-sectional images of the whole restored cavity were obtained by SS-OCT, to which locations the specimens were later trimmed, polished and observed under CLSM. Other specimens were prepared and scanned by OCT followed by MTBS testing.

[Results]: Increased SS-OCT signal intensity along the interface corresponded well to the interfacial gaps detected by CLSM. There was a significant correlation between MTBS and Adaption at cavity floor. SEM images demonstrated different failure modes for the tested MTBS specimens.

[Conclusion]: SS-OCT imaging technology can be used to non-invasively detect and quantify micrometer gaps at the bottom of composite restorations. In addition, it can provide information on the performance and effectiveness of dental composites.

DEDICATION

DEDICATION

This work is dedicated to the great source of inspiration and motivation, my father Prof. Abdulsalam BAKHSH, mother Fawziyah DAHLAWI, my brothers and sisters.

Also, I dedicate this work to my friends for their countless support and assistance.

Lastly and most importantly, I dedicate this work to my darling wife Dr. Mona MANDURAH and beloved daughter Lamar and son Abdullah, for their never-ending love, understanding and support.

AKNOWLEDGMENTS

AKNOWLEDGMENTS

I would like to express my heartfelt gratitude and appreciation to the Chairman of Cariology and Operative Dentistry, Oral Restitution Department, the program promoter **Prof. Junji TAGAMI**, who always inspires me not only to get insights into science, but also to gain knowledge outside science. I am deeply indebted to Dr. M. OTSUKI, Dr. S. NAKASHIMA, Dr. T. NIKAIDO, Dr. M. NAKAJIMA, Dr. Y. KITASAKO, Dr. T. YOSHIKAWA, Dr. G. INOUE, Dr. E. CHO, Dr. K. HOSAKA, Dr. T. TAKAGAKI, Dr. N. SEKI, Dr. R. TAKAHASHI, Dr. H. HAMBA, Dr. ARAMAKI, Dr. K. MATIN and Dr. A. BAKRY for their encouragement and extensive logistical support. Also, I am very thankful to **Dr. Y. SHIMADA,** my co-Adviser for his kind encouragement, motivation, help, support and guidance during my study period in TMDU.

I would like to address a special acknowledgment for my mentor and main Adviser **Dr. Alireza SADR**, Junior Associate Professor at Tokyo Medical and Dental University and Chaperon in Global–COE, for his patience and unlimited guidance in helping me to get into the academic research, for his unconditional support, and for providing me the opportunity to conduct research in different field of adhesive dentistry

under his constructive comments. His creative guidance and endless dedication gave me great motivation to think differently. His encouragement, enthusiasm, and everlasting friendship made my graduate training at Tokyo Medical and Dental University a memorable and meaningful experience. I learned a lot from him; inside and outside the campus, and he was one of the most influencing people in my life. I will never be able to thank him enough and show him how much I respect and appreciate him and all he has.

I would also like to express my sincere appreciation to all my friends and family especially my dad, mom, brothers and sisters, Dr. Particia MAKISHI, Dr. Yuko NATSUME, Dr. Ilnaz HARIRI Dr. Hamid NURROHMAN, Dr. Amir NAZARI, Dr. Prasansuttiporn TAWEESAK, Dr. Suppason THITTHAWEERAT, Dr. Gerardo MENDEZ, Dr. Sofiqul ISLAM, Dr. Ena LODHA, Dr. Mohannad NASSAR, Dr. Ornicha THANATVARAKORN, Dr. Alaa TURKISTANI, Dr. Sahar KHUNKAR, Dr. Ehab AL-SAYED, Dr. Baba BISTA, Dr. Aidil ZUEAKMAL, Dr. Maja ROMERO, Dr. Ikumi WADA, Dr. Zaher BUKHARI, Hisaichi NAKAGAWA and my colleagues in TMDU student Chapter, and all the people in this department, for their friendship and invaluable participation in scientific discussions and generous support.

My sincere acknowledgement is extended to the Royal Government of Saudi Arabia and King Abdulaziz University for giving me the opportunity to peruse my postgraduate studies in Japan. Also, my acknowledgments to Prof. Fadel Osman, Dr. Hanadi MARGHLANI and Conservative Dentistry department's members in KAU for their support.

Furthermore, my cordial acknowledgment to the Ambassador Dr. Abdulaziz TURKISTANI, the Cultural Attaché Dr. Essam BUKHARI as well as to my colleagues in Royal Embassy of SAUDI ARABIA, for their warmest encouragement and support and tremendous help during my stay in Japan.

Moreover, my great appreciation to the companies that provided dental materials and equipment used in the experiments, especially, Kuraray Noritake Dental, Tokuyama Dental, Santec and Panasonic Healthcare.

Finally, a special thanks goes to my lovely wife Mona MANDURAH and my beloved children and to all those people who I failed to mention here, but in one way or another have been an inspiration to me and provided utmost assistance, I sincerely thank you all.

PREFACE

PREFACE

This thesis is based on the original research works by the author, to which the following articles refer:

Article 1.   **Bakhsh TA**, Sadr A, Shimada Y, Tagami J, Sumi Y. Non-invasive quantification of resin-dentin interfacial gaps using optical coherence tomography: Validation against confocal microscopy. Dent Mater 2011;27:915-25.

Article 2.   **Bakhsh TA**, Sadr A, Shimada Y, Khunkar S, Tagami J, Sumi Y. Relationship between Non-destructive OCT Evaluation of Resins Composites and Bond Strength in a Cavity. Proc. SPIE 2012;8208:820809.

Article 3.   **Bakhsh TA**, Sadr A, Shimada Y, Mandurah M, Hariri I, Alsayed E, Tagami J, Sumi Y. Concurrent Evaluation of Composite Internal Adaptation and Bond Strength in a Class-I Cavity. J Dent. Oct 2012. Doi:10.1016/j.jdent.2012.10.003.

TABLE OF CONTENTS

CONTENTS

LIST OF TABLES

LIST OF TABLES

Table

LIST OF FIGURES

LIST OF FIGURES

CHAPTER 1

CHAPTER 1

1.   BACKGROUND AND LITERATURE REVIEW

The realized need for high-resolution real-time functional biomedical imaging techniques has prompted investigative efforts to refine imaging modalities for dental applications. Optical coherence tomography (OCT) is an emerging optical technology in biomedical optics and medicine. It implements high resolution, volumetric and cross-sectional tomographic imaging of the internal microstructure in materials and biological tissues by measuring echoes of backscattered light [1]. This powerful imaging technology can obtain "optical biopsy" in real time, permitting *in situ* visualization of tissue microstructure, without the need to remove and process specimens [2]. Moreover, when the OCT is coupled with catheter, endoscopic, laparoscopic, or needle delivery devices, it has a powerful impact on many medical applications ranging from the diagnosis of neoplasia, to enabling new minimally invasive surgical procedures. The unique features of OCT makes it a powerful imaging modality, which promises to enable many fundamental research and clinical applications [2].

Early OCT imaging engines employed time-domain detection with an interferometer using a low-coherence light source and scanning reference delay arm. It performs cross-sectional imaging by measuring the magnitude and echo time delay of backscattered light. Cross-sectional images generated by performing multiple axial measurements of echo time delay (axial scans or A-scans) and scanning the incident optical beam transversely. This generates a two-dimensional data set, which represents the optical backscattering in a cross-sectional plane through the tissue. Images or B-scans can be displayed in a false color or grey scale to visualize tissue changes. Acquiring serial cross-sectional images by scanning the incident light beam in a raster pattern can produce three-dimensional, volumetric data sets (Figure-1). Three-dimensional OCT (3D-OCT) data contain comprehensive volumetric structural information and can be manipulated similar to Magnetic Resonance (MR) or Computed Tomography (CT) images [1]. The majority of earlier OCT imaging systems was based on the principles of time-domain low-coherence interferometry. This includes the development of a polarized-sensitive OCT (PS-OCT). Recently, OCT technology has greatly advanced by the development of spectral discrimination techniques, which provide a substantial increase in sensitivity over traditional time-domain OCT.

Swept source OCT (SS-OCT) is one of the most recent implements of the spectral discrimination, using a wavelength-tuned laser as the light source and providing improved imaging resolution and scanning speed [3, 4].

A number of comparisons and contrasts can be made between OCT and these other in-depth imaging modalities; ultrasound and confocal microscopy, in term of resolution and imaging depth (Figure-2). Ultrasound imaging has a typical resolution ranging between 0.1-1 mm and depends on the sound wave frequency (3-40 MHz) used for imaging and these waves are transmitted with minimal absorption in biological tissues that makes it possible to image deeper area. Alternatively, confocal microscopy has an extremely high resolution up to 1 µm. However, the imaging depth in biological tissue is limited due to the signal loss and limited focal range. Imaging depth, which is up to a few hundred micrometers, is also significantly degraded by optical scattering [5].
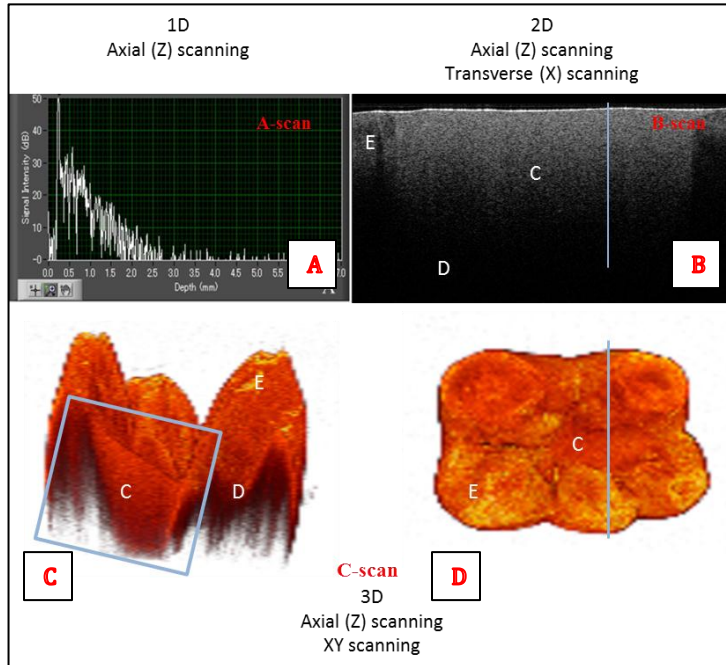
Figure-1:

OCT generates cross-sectional; or three-dimensional images by measuring the magnitude and echo time delay of light. (A) Axial scans (A-scan) measures the backreflection or backscattering versus depth. (B) Cross-sectional image for a restored class-I cavity can be generated by performing a series of axial scans at different transverse positions to generate a two-dimensional data set (B-scan), which is displayed as a grey scale or false color image. The blue line is indicating a single A-scan. (C) Cross-sectional image for a restored human tooth in 3D mode for the same location. (D) Three-dimensional data set (C-scan or 3D OCT) can be generated by raster scanning a series of two-dimensional data sets (B-scan). C: Composite; E: Enamel; D: Dentin. (3D image generated by OCT Viewer v. 2.0)

OCT is an interferometric technique, typically employing near-infrared light. Unlike ultrasound, the axial resolution in OCT is determined by the bandwidth of the light source that is ranging 1-15 µm, approximately 10-100 times finer than standard ultrasound imaging. In ophthalmology, it has become a clinical standard because it is still the only method that can perform non-invasive imaging with these resolutions. However, the main disadvantage of OCT is imaging depth that is limited to a few millimeters, typically ~2 mm; due to the scattering effect of the light by most biological tissues [3]. The first application of OCT in the biomedical field was for human retina *ex vivo* imaging by Huang et al in 1991. In 1998, the first *in vitro* images of porcine dental tissues were reported, and subsequently *in vivo* imaging of human dental tissues proved that OCT could be used as a valuable diagnostic aid for several applications within dental medicine. The goal of dental OCT is to produce *in vivo* images of dental microstructure that can be used to make both qualitative and quantitative assessments of oral tissue. This includes buccal diseases as well as dental restoration defects [3].

Since the introduction of acid etching technique by Buonocore (1955), Bis-GMA by Bowen (1962) and total-etch system by Fusayama

(1979), resin-based dental materials are becoming widely popular among the practitioners, patients and health policy makers. In principle, dental composites comprise of three main components; an organic resin matrix, filler particles (mainly containing silica) and a silane-coupling agent that binds the two former components. Other ingredients include polymerization initiators, pigments and stabilizers. These materials are bonded to the dental structure using special and sophisticated resin-based adhesives; etch and rinse and self-etch adhesives systems. Unlike amalgams and other metallic materials, resin-based restorations can develop strong adhesion to the dental tissue. Moreover, the newly developed composites show higher mechanical strength and better esthetics compared to glass ionomer materials. These facts have made them the material of choice for minimally invasive (MI) treatments. The MI concept advocates the least possible amount of tissue removal while preparing the tooth for placement of the restoration, and relies on the adhesion of material to enamel and dentin [6].

In spite of superior aesthetic quality, simple operation technique, and enhanced mechanical strength, the composite materials still suffer a few shortcomings; most of composite materials based on Bis-GMA

undergo volumetric polymerization shrinkage. The shrinkage of composites depends on their resin compositions, degree of conversion, filler type and filler concentration. This shrinkage phenomenon is a result of the conversion of the monomer molecules into a long cross-linked polymer network that generates stresses at tooth-restoration interface. However, with the recent advances in nanotechnology and nanomaterials, it is postulated that mechanical properties and polymerization shrinkage of dental composites can be significantly improved [6, 7].

Nanotechnology is widely considered to be the latest key technology and becoming increasingly linked with advances in biotechnology. By definition, nanostructure means an atomic, molecular structure that has at least one physical dimension of approximately 1-100 nanometers; and possesses a special property, provides a special function, or produces a special effect that is uniquely attributable to the structure's nanoscale physical size [7]. In dentistry, there are considerable recent interests in developing new dental composites formula that are reinforced with nano-sized particles with near-zero shrinkage rates and volumetric shrinkage during curing. However, when the polymerization contraction stress exceeds the bond

strength to the cavity walls, interfacial seal is lost and leads to gap formation [8].
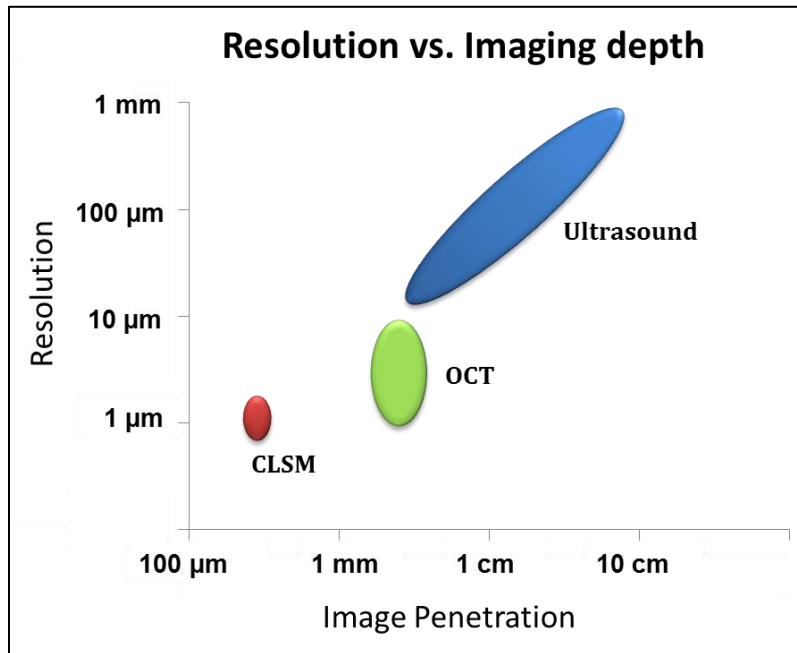
Figure-2:

Comparison of resolution and imaging depth for ultrasound, OCT and confocal laser microscope. Unlike the ultrasound, which can image deep structure, the axial resolution of in OCT modality is ranging from 1-15 μm and is determined by the coherent length of the light source. In most biological tissues the imaging depth is limited to 2-3 mm by attenuation from optical scattering. Confocal microscopy has submicron resolution, but optical scattering limits the imaging depth to a few hundred micrometers in most tissues. (Courtesy of W. Drexler and J. Fujimoto)

Regardless of the cause, such microgaps will potentially result in failure of restorative treatment due to hypersensitivity of the restored vital tooth, bacterial microleakage, secondary caries or debonding; and thus is critical in the success of the restoration (Figure-3). Several studies reported about the size of these gaps, ranging from 0.3 μm up to 16 μm. Such loss of interfacial seal is undetectable by the conventional methods; radiographs and clinical modules. Several investigators consider these polymer-based resin-filled restorations as a challenging and interesting substrate to be investigated, because of the highly scattering composition [9]. Additionally, studying the interaction of light within such biomaterial bonded to a tooth will add an additional excitement and makes it more clinically relevant.

A conventional SS-OCT was able to identify the defects and gaps at the tooth-restoration interface with axial cavity imaging depths up to 1.7 mm as an increased backscatter intensity value. The difference in backscatter intensity signal suggested to be caused by the contrast between the refractive properties of enamel, dentin, resin and or the medium filling the microgaps, such as air or fluids [3]. An interfacial-sealing test based on this phenomenon was the core methodology to perform the experiments included in this dissertation, and will be

discussed in more details in the next chapter. A schematic illustration of

the SS-OCT system is presented in figure-4.
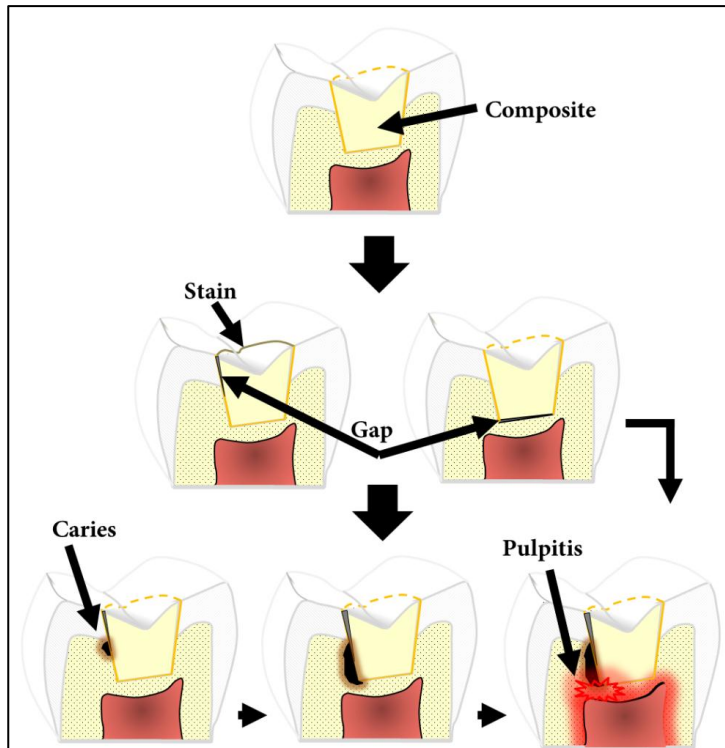
Figure-3:

**Dental composite, microleakage and the possible associated
complications with the loss of interfacial seal.**
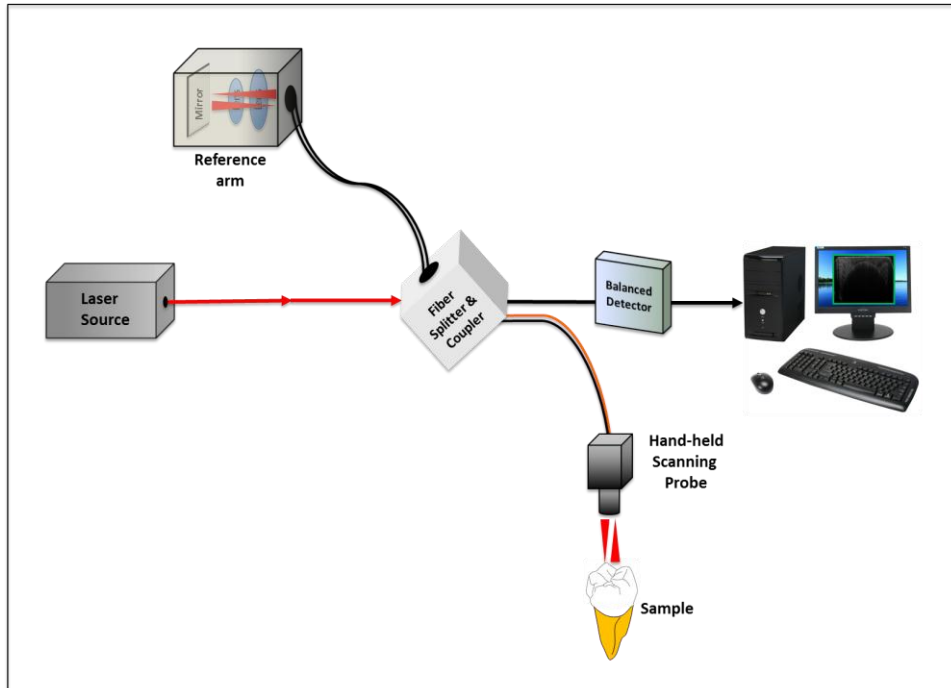
Figure-4:

The light output from a high-speed scanning laser is divided into sample arm and reference arm by a beam splitter. Reference light and back-scattered light from the sample are recombined together to create the interferogram in time. Fringe response is detected with a balanced detector, converted to electrical signal and digitized by analogue-to-digital (A/D) board. Software constructs a 2D image from the signal after Fourier transform.

Chapter 2 demonstrates a non-invasive method to convert and analyze the OCT date quantitatively using image analysis software through several image-processing steps. It was investigated whether an

increased SS-OCT signal intensity along the interface corresponded to the interfacial gaps detected by CLSM.

That first research has risen up other topics to be researched within the field of advanced light technology. Loss of the interfacial seal, that may be complicated with gram negative bacterial invasion, secondary caries development and teeth hypersensitivity in some restored teeth with resin based restorations, directed the trend of research toward investigating the factors that may cause these unprecedented complications. One of these factors is the strength of the bond between the tooth-resin complex. It has been reported in the literature that the bond strength at the cavity floor were significantly reduced compared with those measured on flat surface. Cavity configurations, volume of materials and filling techniques have greater influence on the marginal seal adaptation and the bonding strength. Many researchers concluded in their results that incremental filing techniques, in comparison to bulk filling technique, are capable of reducing the concentration of stresses at the tooth-composite interface and as a consequence minimal liability of gap formation [8]. For nanotechnology-based composites, an improvement in physical properties is expected due to the increased interfacial interactions

between resin and fillers, which in turns will have a great influence on reduction of the polymerization shrinkage as reported in the literature; however, it was not clear whether these new formulas will alleviate the need for incremental placement.

Micro-tensile bond strength test (MTBS) is a conventional evaluation method of regional bond strength to small areas within tooth substrate. Therefore, it was thought provoking to combine and compare SS-OCT and MTBS in evaluation of the bonding performance and composite adaptation in a clinically relevant circumstance. This will be discussed in more details in chapter 3 and 4.

CHAPTER 2: NON-INVASIVE QUANTIFICATION OF RESIN-DENTIN INTERFACIAL GAPS USING OCT: VALIDATION AGAINST CLSM

NON-INVASIVE QUANTIFICATION OF RESIN-DENTIN INTERFACIAL GAPS USING OPTICAL COHERENCE TOMOGRAPHY: VALIDATION AGAINST CONFOCAL MICROSCOPY

2.1. INTRODUCTION AND OBJECTIVES

Gaps and lack of integrity at the tooth-restoration interface may affect the success of an adhesive restoration. The loss of interfacial seal may result in bacterial microleakage, secondary caries and hypersensitivity of the restored vital tooth, eventually leading to failure of the treatment [10, 11].

Most of the composite restorations suffer from volumetric polymerization shrinkage [12, 13]. This shrinkage phenomenon generates stresses at tooth-restoration interface that might weaken the restoration integrity, and lead to gap formation. Low adaptation to the cavity might also be the result of the low bonding performance of the

adhesive, relatively high stiffness of the uncured composite during placement [13] or insufficient copolymerization of adhesive and bonding agent [14, 15].

Detection of these micro-defects is important both from the clinical point of view and in dental materials research. It was reported that the gaps mainly occur at the line-angles or at the cavity base, and range from less than a micrometer up to several tens of micrometers in size [16, 17]. They are undetectable by the conventional diagnostic methods, such as radiographic films, which suffer from image superimposition and lack of accuracy on the micron-scale [18]. Conventionally, dye-penetration leakage tests and microscopic assessment of the interface have been employed for *in vitro* detection of these interfacial gaps. Those methods are highly subjective, and require sectioning of the teeth to evaluate the interface, which make such destructive techniques unsuitable. These disadvantages led to incorporation of newer diagnostic technologies for research on adaptation of restoration, such as 3D imaging by X-ray micro computed tomography (micro-CT) [16, 17, 19, 20].

Recently, optical coherence tomography (OCT) was addressed as a non-invasive cross-sectional imaging of the internal biological system

24

at the submicron scale [1]. It is a promising imaging modality, which does not require cutting and processing of the specimens and allows the visualization of microstructures of tissue and biomaterials in the real-time [1, 21].

OCT was developed based on the concept of low-coherence interferometry. In simple words, a laser source is projected over a sample, and the backscattered signal intensity from within the scattering medium reveals depth-resolved information about scattering and reflection of the light in the sample. The signal from serial scans can be transformed into an image by a software [1].

It has been reported in the literature that the first application of low-coherence interferometry in the biomedical optics field was for the eye length measurement by Fercher *et al,* in 1988. Nowadays, OCT is being used as a clinical diagnostic modality in various medical fields [22]. In dentistry, the first series of reports about imaging of the dental hard and soft tissues appeared in the late 1998's. [23-25]. Afterwards, several researchers used different types of OCT systems for research and diagnosis of dental diseases, including periodontal diseases and early caries lesions [26, 27]. The majority of earlier OCT imaging systems were based on the principles of time-domain low-coherence

interferometry. OCT technology has greatly advanced in recent years by the development of spectral discrimination techniques, which provide a substantial increase in sensitivity over traditional time-domain OCT. SS-OCT is one of the most recent implements of the spectral discrimination, using a wavelength-tuned laser as the light source and providing improved imaging resolution and scanning speed [28].

Some studies have pointed out the potential of OCT for investigation of the gap formation at tooth-restoration interface [29, 30]. However, to our knowledge, few reports have been published in the dental literature focusing on the method development for quantitative gap measurement at the tooth-composite interface using OCT, and validating the results with a common destructive microscopic technique.

In this study, we examined the tooth-composite restoration interface at the cavity floor of the restored teeth by SS-OCT and compared the findings with confocal scanning laser microscope (CLSM). The hypotheses in this study were that an increased OCT signal intensity at the cavity floor under composites indicated existence of interfacial gap, and that this area of increased signal intensity represented gap size, both in length and height.

2.2. MATERIAL AND METHODS

2.2.1. MATERIALS USED

The materials used in this study are listed in Table-1. The lot number and chemical composition of each material are according to the information provided by the manufacturer (Kuraray Noritake Dental, Tokyo, Japan). Three composite resins were evaluated in this study; Clearfil Majesty Posterior (MJ-POST) is a posterior composite with high nanofiller content, Clearfil AP-X (APX) is a conventional hybrid composite restoration and Clearfil Majesty LV (MJ-LV) is a high filler-loaded flowable composite. An all-in-one self-etching adhesive system, Clearfil Tri-S Bond was used in combination with each one of the composite resins in this experiment.

2.2.2. RESTORATIVE PROCEDURE

The experimental design of this study and the use of extracted human teeth were subjected to the guideline of the Ethics Committee of Tokyo Medical and Dental University.

Twenty-one caries-free human premolar teeth were used in this study. After cleaning with a dental scaler, the occlusal cusps were grounded to obtain a flat occlusal table in enamel using a model

27

trimmer, and then polished with 600-grit silicon carbide papers (Sankyo Rikagaku, Saitma, Japan). The roots of the teeth were cut away, and the remaining coronal portions were trimmed into a block shape with the parallel opposing walls (buccal, lingual, mesial and distal) perpendicular to the occlusal and cervical walls. A standard cylindrical class-I cavity with the floor located in dentin, 3 mm in diameter and 1.5 mm in depth was prepared using a flat-end tapered diamond bur (SB2, GC, Tokyo, Japan) attached to an air turbine headpiece under copious cooling water. Clearfil Tri-S Bond was used according to the manufacturer's instructions. It was applied on the cavity surface for 20 seconds, dried with gentle air pressure for 5 seconds and irradiated with a halogen light-curing unit (Optilux 501, Kerr, CA, USA; 550 mW/cm^2) for 10 seconds. The teeth were divided into 3 groups according to the study design (MJ-POST, APX and MJ-LV) with 7 teeth in each group. The cavities group were filled with the corresponding composite following the bulk-filling technique and then light-cured for 40 seconds. A schematic drawing for the sample preparation and visualization under the SS-OCT and CLSM is showed in Figure-5a.
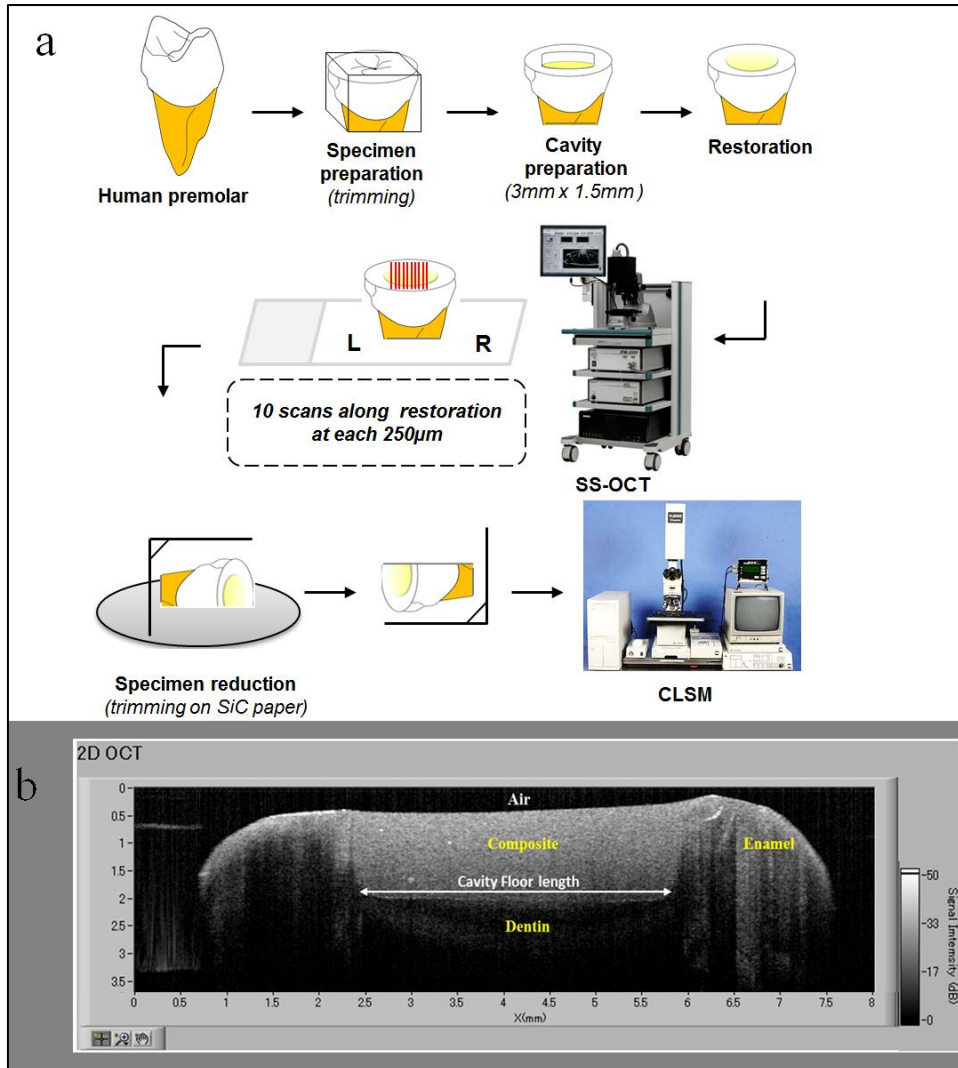
Figure-5:

(a) Schematic drawing for the sample preparation and visualization under the SS-OCT and CLSM. Each of the human premolars was subjected to trimming of occlusal surface and sides (specimen preparation) and cavity preparation. Resin composite was applied using bulk filling technique and according to the manufacturer instructions after application of the adhesive material. Then, 10 serial scans were obtained for each sample under the SS-OCT. Before CLSM observation,

the samples were subjected for trimming and polishing with silicon carbide paper and diamond paste under copious cooling water. (b): B-scan image obtained from the SS-OCT. The dimensional parameter (length of the cavity) that was discussed in this study is showed on this OCT B-scan image.

2.2.3. OCT SYSTEM

The SS-OCT system (OCT-2000®, Santec, Komaki, Japan) used in this study had the same setup components as described by Shimada *et al*. [26]]. It is a frequency domain OCT system integrating a high-speed frequency swept external cavity laser, of which the probe power is less than 20mW, within the safety limits defined by American National Standards Institute. The light source in this system sweeps the wavelength from 1260 nm to 1360 nm at 20 kHz sweep rate with central wavelength at 1319 nm. The axial resolution of this OCT system is 11 μm in air, which corresponds to approximately 7 μm within a biomedical structure with a refractive index of around 1.5. The lateral resolution of 17 μm is determined by the objective lens at the probe. The focused light-source beam is projected onto the sample and scanned across the area of interest in two dimensions (x, z) using a hand-held probe. Backscattered light from the sample is returned to the

system, digitized in time scale and then analyzed in the Fourier domain to reveal the depth-resolved reflectivity profile (A-scan) at each point.

The combination of a series of A-scans along the section of interest creates a raw data file (B-scan) with information on the signal intensity (backscattered light) and x, z coordinates from each point within the scanned area. Two-dimensional cross-sectional images can be created by converting the B-scan raw data into a gray-scale image [26, 31].

2.2.4. CROSS-SECTIONAL VIEWING OF THE CAVITIES USING CLSM

Direct observation of the interface in the sample under CLSM (1LM21H/W, Lasertec Co., Yokohama, Japan) was accomplished after trimming off the labial wall of the sample up to the cross-section that was previously imaged by SS-OCT. The trimming was done with different sizes of silicon carbide paper ranging from 280-grit up to 2000-grit in an ascending sequence and the specimens were further polished with diamond paste down to a particle size of ¼ μm in circular motion under copious cooling water. The cavity floor on each cross-section was imaged at (1250×) magnifications.

Table-1: Composites resins and adhesive system used in this study.

Material (Manufacturer) Code	Ingredients	Lot No.	Shrinkage*	Composite filler content (Weight %) **
Clearfil Majesty Posterior composite restoration (Kuraray Noritake, Japan) MJ-POST	• Bis-GMA • TEGDMA • Silanted silica filler • Silanated glass ceramics • Surface treated alumina micro- filler • Hydrophobic aromatic dimethacrylate • Others	00107B	1.5% (Volumetric)	91
Clearfil AP-X composite restoration (Kuraray Noritake, Japan) APX	• TEGDMA • Bis-GMA • Silanted barium glass • Silanated colloidal silica • Silanated silica • Others	01044A	1.24% (Linear)	85
Clearfil Majesty LV Flowable composite (Kuraray Noritake, Japan) MJ-LV	• TEGDMA • Silanated barium glass powder • Silanted colloidal silica • Hydrophobic aromatic dimethacrylate • Others	00214A	1.88% (Linear)	81
Tri-S bond All-in-One Light-cured Adhesive System (Kuraray Noritake, Japan) Tri-S	• Bis-GMA • MDP • HEMA • Ethanol • Water • Photoinitiators • Silanted colloidal silica	00133A		-

Abbreviations: TEGDMA: Triethylene-glycol dimethacrylate; Bis-GMA: Bisphenol Adiglycidyl ether dimethacrylate; MDP: Methacryloyloxydecyldihydrogen-phosphate; HEMA: 2-hydroxylethyl methacrylate. *, ** Data as disclosed by the manufacturer.

2.2.5. IMAGE ANALYSIS

A.   OCT DATA

SS-OCT raw B-scan data were imported to an image analysis software (ImageJ ver. 1.42q) [32] to detect significant increase in the signal intensity at the resin-dentin interface at the cavity floor. The higher signal intensity appeared as bright clusters formed by bright pixels at the interface. In order to calculate the size of those bright clusters, an image analysis procedure was followed; the size scale was set, and the image was subjected to a median filter (1 px radius) to reduce the noise. The median filter is a non-linear digital filtering technique, often used to remove noise as a typical pre-processing and widely used step to improve the results of later processing. Median filtering is very in digital image processing because under certain conditions, it preserves edges while removing noise [33]. These steps were performed by a plug-in compiled for the software. The image was then cropped to the area including the cavity floor in the center, of which the height was 500 μm (optical), and the width was equal to that of the cavity floor according to the location of the slice. The cropped image of the cavity floor was subjected to the binarization process according to the Isodata algorithm [33] in the auto-threshold function of the software to determine the target pixels with significantly higher brightness

compared to other pixels in the background. Image binarization converts a grayscale image to a binary image (bi-level or black and white image), using a certain threshold (cut-off range) to visualize important information in an image. In an automated binarization process, the target image is produced base on a threshold determined automatically using an algorithm. On the binary image, the length of each bright cluster along the cavity floor was calculated. Average height of each cluster was calculated by dividing the length of each cluster on the total area of that cluster.

Bright cluster length percentage of the cavity floor on each cross-section was calculated according to the following equation:

Bright clusters length % = $\frac{total\ length\ of\ bright\ clusters\ at\ each\ slice}{length\ of\ the\ cavity\ floor\ at\ that\ slice} \times 100$

The number of slices, which showed no detectable brightness at the cavity floor, was also recorded for each composite material. The dimensional parameter (length of the cavity) mentioned in this study is shown in Figure-1b.

B.   CLSM IMAGES

After trimming the specimen to the desired location, the gap dimensions (length and height) in the obtained images at (1250×)

magnification were analyzed using software interfaced to CLSM device (LM eye ver. 2.66). The image analysis procedure was as follows; setting the size scale for measurements, cropping the de-bonded interfacial area, outlining the gap area manually, and measuring the gap length along the cavity floor directly. The average height of each gap was calculated through dividing the area of each gap by the length of that gap.

2.2.6. STATISTICAL ANALYSIS

Statistical analysis of the results was performed using a statistical software package (Dr SPSS-2 for windows: SPSS Inc., Chicago, IL, USA). In order to determine a relationship between the bright cluster (corresponding to increased OCT signal intensity) and actual gap size (height and length according to CLSM), the results were subjected to Pearson's correlation and linear regressions, with the significance defined as ($p < 0.05$).

After examining the correlation between the OCT bright cluster length and CLSM actual gap length, the results were compared between the different composite materials. The test variable was bright cluster length percentage, which corresponded to the gap percentage at cavity floor. The values obtained from the cross-sections on each cavity were averaged and a single value per tooth was included in the statistical analysis. Since the

distribution of data was not normal, non-parametric tests were performed. Kruskal-Wallis test was used to determine whether there was any difference between materials, and Mann-Whitney U-test after Bonferroni correction was used for pairwise comparisons comparison between each two materials.

2.3. RESULTS

Figures (6-8) show typical B-scan images obtained by the SS-OCT and cross-sections as confirmed by the CLSM for each group. The B-scan images of the MJ-POST sample showed white clusters at several areas of the cavity floor. Observation by the CLSM for the same sections indicated that these white clusters (formed due to increased intensity of backscattered light) correspond to interfacial gaps (Figure-6). For APX and MJ-LV samples, the same phenomena were observed in the B-scan images, which were later confirmed by the CLSM as interfacial gaps (Figures-7, 8). For the gap length measurements, a significant correlation was found between the length of the cluster with brighter pixels along the cavity floor from the SS-OCT, and the actual length of the gap at the corresponding location as measured under the CLSM (Pearson correlation coefficient r = 0.970, p < 0.001). A significant linear regression was also found between the two measurements (R^2 = 0.984, p < 0.001) (Figure-9A), indicating that the bright clusters indeed

represented gap at the cavity floor. On the other hand, when the relationship between the height of bright cluster and gap height was analyzed, no significant correlation was found ($r = 0.205$, $p > 0.05$) (Figure-9B).

Comparison of bright cluster length percentage (gap length percentage) at the cavity floor between different composites showed significant difference between groups ($p < 0.01$) as presented in Table-2. Pairwise comparisons indicated that APX group showed significantly different gap formation compared to the other two composites ($p < 0.01$), while there was no statistical difference between MJ-POST and MJ-LV composites groups ($p > 0.05$). In APX group, which showed the lowest mean rank, 37% of the B-scan images showed no bright cluster (equivalent to gap free cross-sections, as confirmed by the CLSM).

Figure-6:

Images obtained for a restored cavity with MJ-POST composite restoration. C is the composite restoration, E shows enamel and D is dentin. Blank arrows with numbers point to the same areas on different images. (a): OCT image after 24 hours; some area of the cavity floor showed distinct white clusters (1). These white clusters formed due to increased intensity of backscattered light represent Fresnel reflection, f̂ points to surface Fresnel reflection. (á): binary image corresponding to interfacial segment of (a); after applying the binarization process to the image reconstructed from the raw data, the pixels at the white clusters on OCT image were converted to black pixels (1), and any other pixels were considered as the background (2). There was a significant correlation between the gap length measurements indicating that the

38

bright clusters indeed represented gap at the cavity floor. (b): the CLSM image corresponding to interfacial area (1). A gap is clearly observed under MJ-POST, and seems to have occurred at the interface between the composite-resin and adhesive layer, with a thin adhesive remaining on the dentin. (c): the CLSM image corresponding to interfacial area (2). There is no gap at the interface at this location.

2.4. DISCUSSION

SS-OCT is a high-resolution, cross sectional imaging technique that permits instant non-invasive imaging of the underlying defects in a biological system. It differs from any radiographic imaging technique in that it has no radiation hazards, which makes it safe for the pediatric and pregnant patients. In the current study, the SS-OCT showed a remarkable capability in detection and quantifying microgaps under the restorations non-invasively. In contrast, the dye penetration and ground sectioning methods require slicing and making the entire margin visible for examination.

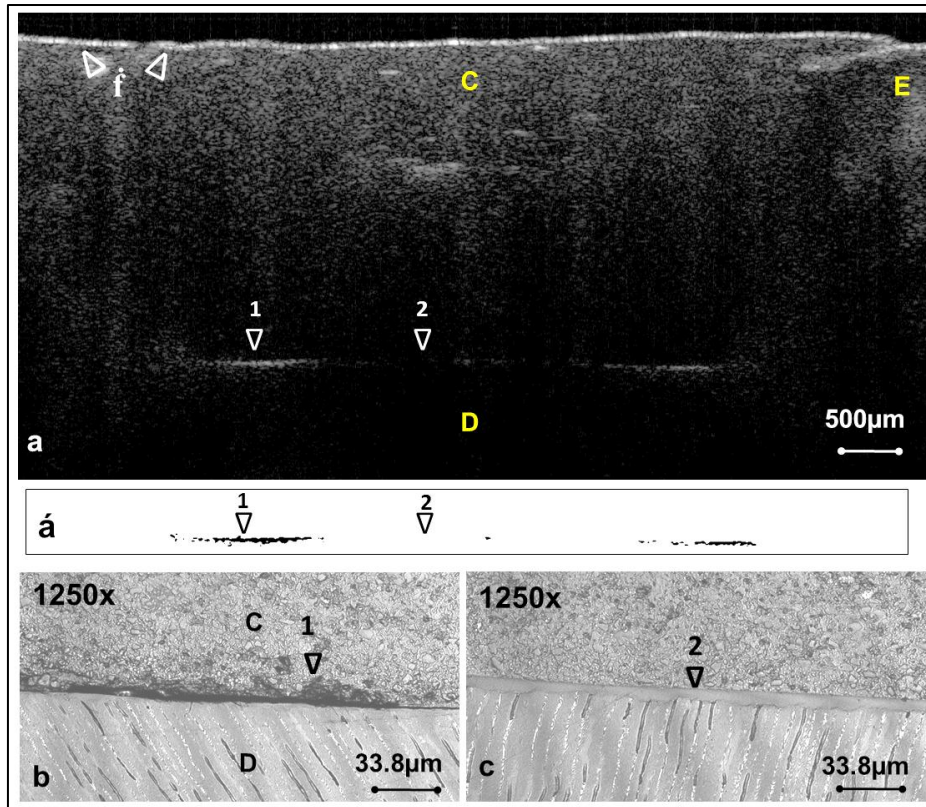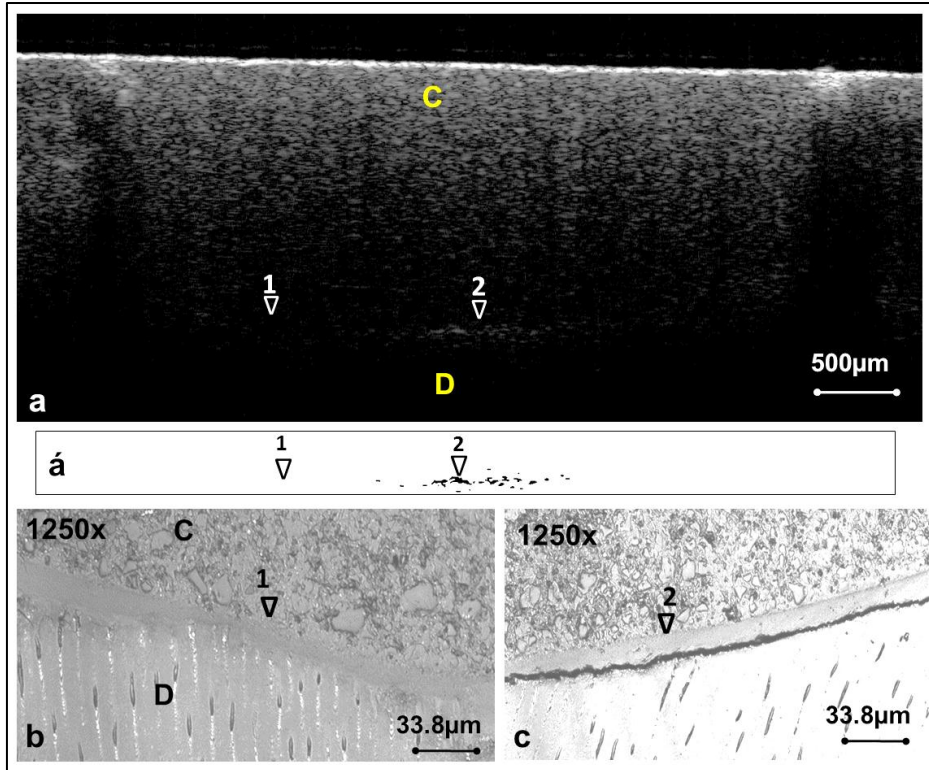**Figure-7:**

Images for a restored cavity with APX composite restoration. C is the composite restoration, and D is dentin. Blank arrows with numbers point to the same areas on different images. (a): SS-OCT B-scan showed the Fresnel effect at the cavity floor at (2). (á): binary image after applying the binarization process. (b): no gap was observed at (1) under CLSM, which corresponds to the results of binary image (á). (c): the interfacial gap location (2) in the cross sectional CLSM image was correlated with the Fresnel effect location in (a) and target pixels in (á). Examination of the CLSM images in APX group indicated the location of the gap was at the adhesive-dentin interface.
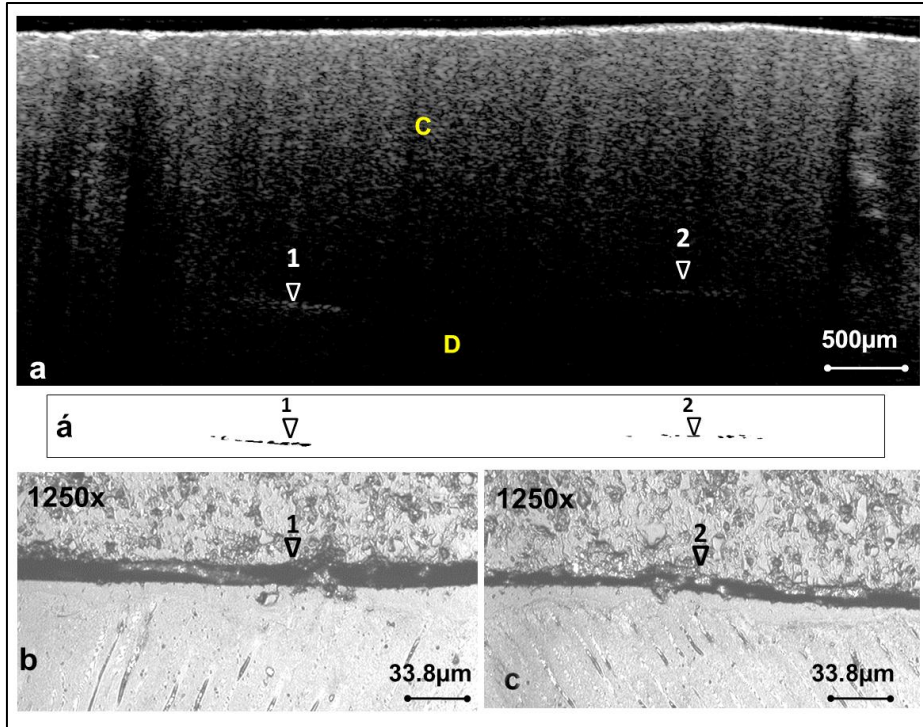
Figure-8:

Images obtained for MJ-LV composite restoration. C is the composite restoration, and D is dentin. Blank arrows with numbers point to the same areas on different images. (a): SS-OCT B-scan showed the Fresnel effect at the cavity floor (2). (á): binary image after applying the binarization process to the interfacial area. (b, c): The interfacial gaps location in the cross sectional images, which obtained by the CLSM were correlated with the Fresnel effect location in (a) and target pixels in (á). Examination under high magnification of the acquired CLSM images revealed that for MJ-LV the gaps were either located at composite-adhesive interface (as in b) or at adhesive-dentin interface (as in both b and c).
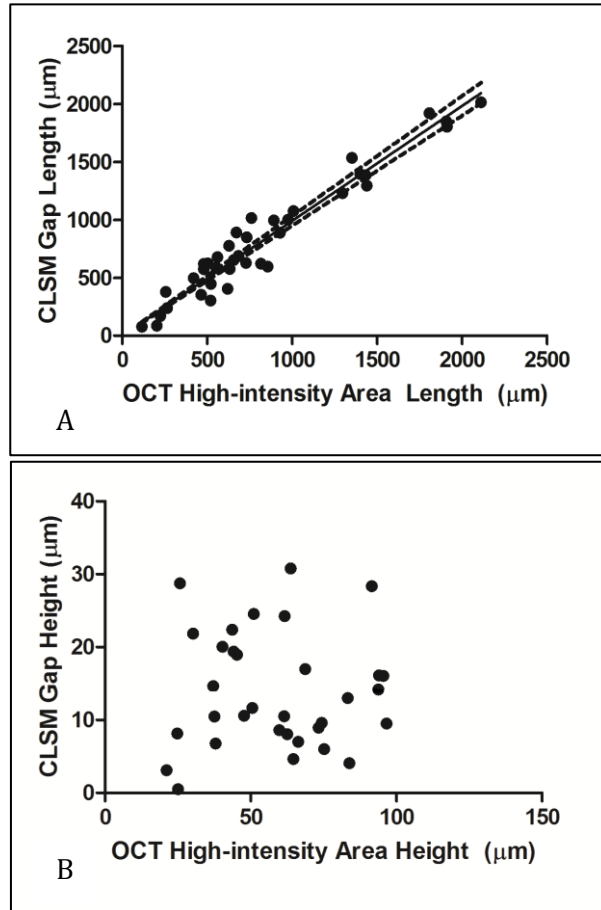
Figure-9:

Graphs representing relationship between OCT and CLSM measurement. (A): gap length regression with 95% confidence intervals. The length of the OCT high-intensity areas was significantly correlated with the gap length measurements from CLSM image (y = 0.99x, r = 0.970, p < 0.001 and R^2 = 0.984 in no intercept model). (B): gap height comparison. The heights of the OCT high intensity areas were not correlated with gaps heights measurement from CLSM images (p > 0.05).

The gaps were studies on 2D cross-sectional OCT images. It was possible to create 3D images from serial SS-OCT 2D image stacks Figure-10a); however, taking into the account the volume of 3D data and lower resolution due to hardware limitation, a series of pilot studies were conducted to determine the minimum number of 2D slices required to evaluate the gaps within each cavity. In the pilot study, serial stacks were obtained during movements of the stage anterio-posteriorly at 750 μm, 500 μm, 250 μm or 100 μm intervals between each two cross-sections. It was found that the results of the latter two measurements were close and therefore, 250 μm interval was selected to obtain the minimum number of 2D slices to evaluate the gap within each cavity. Nevertheless, it should be mentioned that the interfacial defect in a cavity is a 3D phenomenon, and would be best described by 3D analysis. Further development in the data acquisition technology would allow obtaining of the high-resolution large data in a shorter time.

High-resolution 3D imaging of dental structures has been reported by micro-CT imaging. However, when considering the interfacial gaps, detection of the micron-scale gaps is very difficult in micro-CT when compared to SS-OCT due to little difference in radio-

opacity between adhesive and air [34]. Moreover, in comparison to current micro-CT systems, the SS-OCT can perform 3D scans in much shorter times. The time required to perform a 3D scan was about 4 sec, while the time required for micro-CT scanning is in the order of minutes [34, 35].

Generally, the imaging depth of OCT systems has been reported to be in the range of 2-3 mm [26, 34, 35]. In this *in vitro* study, the SS-OCT was utilized to investigate the dentin cavity floor for the presence of interfacial gaps under different types of composites in standard cylindrical class-I cavities.

Our hypothesis was that the change in the signal intensity (small peak) at the interface of resin and dentin, which appeared as bright areas indicated interfacial gap. When light traverses the interface through two different media, it undergoes refraction as well as partial reflection. A Fresnel phenomenon is the reflection of a fraction of light at an interface between two media with different refractive indices, which depends on the incidence angle and refractive index (n) contrast. The refractive index of air, which we assumed was filling the gap, is $n = 1.0$ and that of both the teeth and the resin composites are in the range of $n = 1.5 \sim 1.6$ [36]. Fresnel reflection is clearly observed at the tooth
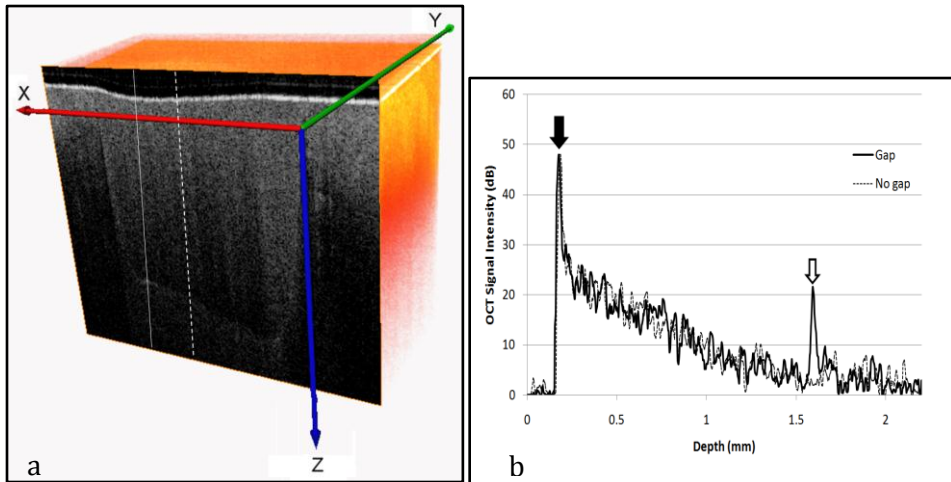
Figure-10:

(a): A 3D SS-OCT scan (512 x 512 x 240 pixels) showing gap formation at the line angles of the restored cavity (Created by Avizo 6.2 3D visualization software). On each cavity, ten high-resolution slices (2001 x 1019 pixels) were analyzed in this study. Signal intensity profiles along the solid white line (crossing bright interfacial area) and dashed white line (crossing dark interfacial area) on the visible 2D slice are presented. (b): SS-OCT signal intensity (A-scan) plotted against corrected depth for the lines in (a). The corrected depth was calculated by dividing the obtained depth from OCT image by the refractive index of the medium, which was 1.5 in this case. The solid arrow shows reflection from the surface of the composite (interface with air) for both line profiles, and the blank arrow points to the second peak indicating reflection from an interfacial gap. Note that no detectable change in signal intensity is observed at those parts of the interface with no gap.

or composite top surface, where the high-intensity light passed through the air-substrate interface (Figure-11b) [27]. In the case the gap is filled

45

with another medium such as water (n = 1.33), the reflections may still exist but would not be as strong as when the air is the medium [34]. Therefore, it should be noted that a higher OCT signal value at an interface might not necessarily indicate existence of a defect, depending on the optical properties of the substances involved. Interpretation of the OCT signal requires knowledge of the optical properties of the media involved, and the interactions of light within the sample. In the case of the composite resin bonded using an adhesive resin to dentin as in the current study, this assumption was valid for the increased intensity appearing as bright sharp clusters at the interface. Attenuation of the light as it penetrates into the structure results in a weaker signal intensity at the 1.5 mm depth within the composite; with such a low signal level at the deep regions, the Fresnel reflection was clearly observed at the interfacial areas (Figure-11b), and the binarization process could outline the areas with intensified backscatter signal intensity (or bright pixel clusters on the image). These clusters were variable in size (length and height) at the interface, and also in the extent of brightness.

Considering the complexity of OCT signal processing as discussed later, the analysis technique described here applies to the particular cavity design and restoration parameters; further studies are needed to investigate the quantifying techniques in cavities with irregular shapes. In this report, a relatively flat cavity floor was investigated, where the light beam is perpendicular to the interface and the interfacial gap was measured along the cavity floor at a constant

depth from the surface. The binarization step was applied only to the cropped interfacial area and not to the entire image, to remove the impact of the higher signal levels associated with the superficial parts of the composite on the binarization process. Further investigation will be conducted to assess the interfacial gaps at the lateral walls of the cavity. Defining a constant threshold value for the gap or non-gap interfaces would be very complicated since factors such as attenuation of light with depth and unique light scattering and transmittance of each material greatly affect OCT signal intensity. In addition, the intensity of the light reaching a particular depth for any position across the sample is affected by how strongly features directly above that position reflect or randomly scatter the light (*e.g.* surface reflections, voids within the composite, scatters such as fillers, etc.) [33, 37].

A very good correlation was found between the lengths of the bright cluster and the length of gap, which partially confirmed our initial hypothesis that these bright areas represented interfacial gaps. Each of the gaps detected in this study ranged from 26 μm to 1.9 mm in length, and 0.5 μm to 35 μm in height (Figures-9 a, b), as confirmed by CLSM. The slope of regression line for the gap length was very close to 1.0 x, indicating the validity of quantitative gap measurements by SS-

OCT. Meanwhile, the results from the two measurement techniques were not perfectly equal, which may be due to slight difference in the location of the slice, effects of specimen processing for CLSM observation, and higher magnification and resolution of CLSM; the expected minimum detectable gap length or lateral resolution of SS-OCT is 17 µm and that of CLSM is 0.25 µm.

Contrary to the gap length, there was no significant relationship for the gap height. It was not expected that the OCT with an axial resolution of 11 µm would accurately measure gaps that were only a few micrometers in height. However, during our preliminary experiments, some results showed an increase in the vertical dimension of the white cluster and others did not. Therefore, it was proposed to find if this quantification technique would be able to give an indication of the gap dimensions. According to the results, the Fresnel reflection only indicated the presence of a medium with low refractive index at the interface, but gave no clear indication of the vertical size of the gap. These reflections were detected even when the gaps were as small as half a micrometer in height, which is well below the SS-OCT axial optical resolution (11 µm) and vertical dimension of each image pixel (6.48 µm). In the case of such a small gap, the

phenomenon appeared as a bright area with irregular boundaries resulting from double reflection of the light at the defect. On the other hand, if the interfacial gap was large enough in height, e.g. 100 μm, it appeared as an optically dark non-scattering area with sharp and bright top and bottom outlines [34]. As one may expect, the height of such dark area between two distinct lines indicates the gap height on the image.

The observation of the tooth-restoration interface by the CLSM was carried out in this study as a diagnostic validation to examine the presence and dimensions of gaps at the cavity floor. Scanning electron microscope observation was avoided because it requires special preparation, desiccation of the sample and low atmospheric pressure, which might induce artifacts [38]. Direct observation by the CLSM does not require any special preparation for the samples after fine polishing [39]. Similar to a previous report, a dye was not used in the cross-sectional imaging of the interface to avoid artifacts caused by absorption of the dye by the dentin adjacent to the composite [40]. Trimming of the specimen to reach the desired section observed through the OCT was performed manually, to control the section

location precisely and to avoid any damage to the interfacial area from the diamond sawing discs.

Three different composites were examined in this study from the same manufacturer with similar resin matrix but different filler compositions to evaluate the effect of these differences on the gap formation when restoring a class-I cavity. It was found that the majority of restorations performed did not turn out to be gap-free and perfectly sealed. However, while interpreting the results, one should be aware that the experimental design was in line with the aim of the study to validate a novel methodology to detect and quantify interfacial gaps. The adhesive material plays a major role in adaptation. An all-in-one adhesive system was chosen in the current study; it was reported that the simplified adhesive showed inferior performance in comparison to the predecessor two-step self-etch adhesive [41].

It is well known that almost any methacrylate-based resin composite undergoes polymerization shrinkage; the extent of shrinkage is widely varied according to the composition and the filler contents [12, 13, 19]. Although a number of studies have shown the effect of increasing filler contents on reduction of the volumetric shrinkage, high filler contents lead to higher modulus of elasticity, which will result in

increased polymerization shrinkage stresses [42-44]. The composites were all placed in the class-I cavity following the bulk technique rather than the widely recommended incremental technique. It is known that bulk filling of a cavity with a high C-factor (such as a class-I cavity used in this study) would reduce the adhesion of composite resin to the cavity floor [45]. In addition, regardless to the type of composite resin, it was found that the shrinkage stress increased as the composite thickness (volume) increased [46].

The MJ-POST is a low-shrinking posterior composite with high mechanical properties and high filler contents, but it showed no better adaptability compared to the flowable composite in this study, MJ-LV. Imaging of MJ-POST samples after placement and before light curing of the composite revealed increased signal intensity at the interface suggesting that the initial adaptation of this composite to the adhesive layer was not complete (Figure-11a), despite operator's efforts to pack the composite well during placement. These reflections generally did not disappear after curing (Figure-11b). In many occasions, CLSM of samples in MJ-POST group showed that the location of gap at the cavity floor was between the composite and the adhesive rather than the dentin-adhesive interface (Figures-11c, d). A previous study [13]

which reported on the lack of integrity at interface between a highly-filled low-shrinkage composite and adhesive suggested that the chemical interaction (*i.e.* polymerization) between adhesive and composite, and the physical adaptation of the composite to the adhesive were both important, with the former being more critical. Such problems as an increased OCT signal intensity at the interface before light curing and bond failure at the composite-adhesive interface were uncommon in APX samples.

The flowable composite evaluated in this study, MJ-LV had also high filler content and mechanical properties comparable to those of the universal composites, showing lower polymerization shrinkage compared to the traditional flowable composites; however, the cavity adaptation achieved with the flowable composite was still inferior to that of the conventional hybrid composite APX in this study. While the flowable composite showed a good initial adaptation (before light curing) under OCT, the CLSM showed that the gaps observed under OCT after polymerization were occasionally due to the loss of integrity at the composite-adhesive interface (Figures-8 b, c). Further improvement in properties of the high-filler content flowable composites, in terms of establishing a balance between shrinkage

stresses, viscosity and wetting capacity, seems necessary to enable their use as suitable composites for bulk filling in deep cavities with high C-factor [38].

In general, these findings confirmed that the adaptation to the cavity floor depended on multiple factors and not only on the volumetric polymerization shrinkage of composites or their filler contents [46, 47]. It is noteworthy that the gap formation at the composite and adhesive resin interface (as observed for MJ-POST and MJ-LV) is likely to make less clinical problems compared to the cases where the dentin seal is completely lost, especially if the adhesive material has the capability to protect dentin against demineralization attack.

Further research is required to investigate these factors in relation to the newly introduced composites with higher filler contents and new chemistries.

SS-OCT has a utility in detecting the gaps before and during polymerization, [48] which will enable distinguishing between gaps generated due to polymerization stress and those arising from lack of adaptability of the resin prior to the light curing.
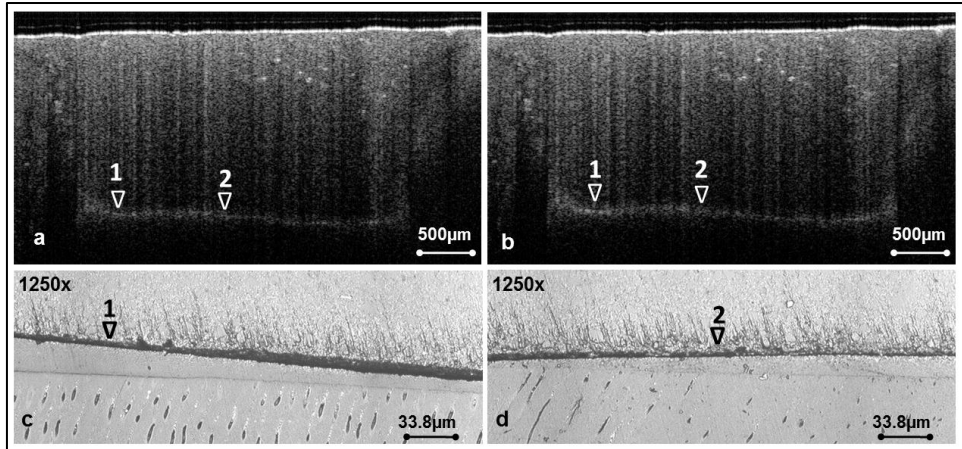
Figure-11:

(a): B-scan image for the composite restoration (MJ-POST) before curing. The cavity floor showed an increase in the signal intensity at the interface of composite resin and cavity floor as shown by white triangle pointers (1, 2). (b): B-scan image for the same cross-section as in (a) after curing. The cavity floor still showed an increase in the signal intensity at the interface of composite resin and cavity floor. (c, d): CLSM images of the same cross-section as in (b) (at 1250x magnification) at locations (1, 2) showing that the gap is formed between adhesive and composite indicating a lack of initial adaptation and/or insufficient copolymerization at the interface.

Table-2: Gap percentage comparison between different composite resins.

Material	Mean Gap % (SD)	Mean Rank of Gap %	Percentage of Gap Free Slices
Maj-Post	52.8 (26.3)	14.43[a]	7.1%
APX	12.4 (10.3)	5.14[b]	37%
Majesty LV	48.0 (27.7)	13.43[a]	5.7%

Values marked by different superscript letters showed a statistically significant difference (Kruskal-Wallis test with Mann-Whitney pair comparison, $p<0.05$).

This technology is also potentially suitable for non-invasive long-term assessment of dental composite restoration defects and durability studies. While imaging depth limitation of this device necessitates further technical development for examination of deeper interfaces, SS-OCT is a promising technology for various laboratory and clinical applications in the dental field.

The first hypothesis of our study was accepted, as the increased signal intensity in the interface represented gap. The second hypothesis, however, was partially accepted as the length of the gap was represented by the length of the white cluster.

2.5. CONCLUSIONS

SS-OCT imaging technology demonstrated a remarkable capability with high sensitivity and accuracy in detection and quantification of few micrometers gaps at the bottom of composite restorations, bearing the potential to become a clinical monitoring and a useful research tool in this field. Adaptation of composites to the cavity floor depended on multiple factors and not only on the polymerization shrinkage of composites or their filler contents.

2.6. ACKNOWLEDGMENT

CHAPTER 3: RELATIONSHIP BETWEEN NON-DESTRUCTIVE OCT EVALUATION OF RESINS COMPOSITES AND BOND STRENGTH IN A CAVITY

CHAPTER 3

RELATIONSHIP BETWEEN NON-DESTRUCTIVE OCT EVALUATION OF RESINS COMPOSITES AND BOND STRENGTH IN A CAVITY

3.1. INTRODUCTION AND OBJECTIVES

In dentistry, tooth-colored direct restorations that are performed by bonding of resin composites to the dental tissue using an adhesive material are increasingly becoming popular. In this regard, rapid development of different restorative materials with improved adhesion to the dental tissues necessitates development of methods that enable laboratory evaluation of the performance of materials in an objective yet clinically relevant way [49]. There are various testing modalities for evaluating the bond strength of dental adhesives and restorative composites to the tooth substrate; microtensile bond strength test (MTBS) is one of the established testing methods, more commonly applied in recent years. Compared to the conventional testing methods, this test takes into account a relatively small adhesive surface area, and

can differentiate well among various adhesives with good bonding performance. MTBS also enables assessment of regional and local adhesion in different restoration and cavity configurations.

In addition to bond strength, restoration-tissue adaptation and interfacial seal evaluation have been introduced as effective methods for comparison of dental restorations. Most of the composite restorations undergo volumetric polymerization shrinkage, which may generate stresses at tooth-restoration interface [3, 50]. This will lead to formation of defects and microgaps under the composite restorations and compromise the adhesion to the dental substrate and restoration durability. Loss of interfacial seal may also be the result of other factors including but not limited to the material compositions, handling properties and technique sensitivity. In addition to factors related to the material, those related to operator and patient also affect the seal and adaptation of a restoration.

While MTBS and adaptation are both recognized as important tests to evaluate the dental composite restorations, up to date, the relationship between cavity adaptation and bond strength is not well understood. Previously, we introduced the potential use of optical coherence tomography in quantification of interfacial gaps in cavity [3,

34, 35]. In this study, we introduce a new testing method to assess cavity adaptation by swept-source optical coherence tomography and MTBS in the same class-I cavity.

3.2. MATERTIALS AND METHODS

3.2.1. MATERIALS USED

The materials used in this study are listed in Table-3. The lot number and chemical composition of each material are according to the information provided by the manufacturer (Tokuyama Dental Corp., Tokyo, Japan). Two composite resins were evaluated in this study; Estelite Sigma Quick (ESQ) is a light-cured, highly spherical nano-filled composite resin. ESQ contains 82% by weight (71% by volume) of silica-zirconia fillers and composite fillers. Palfique Eselite LV (PLV) – medium flow type is a low viscosity, light-cured and high nanofiller-loaded (68% by weight) flowable composite. An all-in-one self-etching adhesive system, Bond force (BF) was used in combination with each one of the composite resins in this experiment.

Table-3: Composites resins and adhesive system used in this study.

Material (Code)	Ingredients	Lot No.
Estelite Sigma Quick Universal Composite (ESQ)	- Bis-GMA - TEGDMA - Silica–zirconia fillers - Silica–titania fillers - Photoinitiators	J018
Universal Composite Flowable Composite (PLV)	- Bis-MPEPP - UDMA - Bis-GMA - TEGDMA, Silica–zirconia fillers - Silica–titania fillers - Photoinitiators	252
Tokuyama Bond Force All-in-One Light Cure Adhesive System (BF)	- Methacryloyloxyalkyl acid phosphate - HEMA - Bis-GMA - TEGDMA - Water - Isopropyl alcohol - Glass fillers - Photoinitiators	059

Abbreviations: HEMA: 2-hydroxyethyl methacrylate; Bis-GMA: bisphenol-A-diglycidyl methacrylate; TEGDMA: triethyleneglycol dimethacrylate; UDMA: urethane dimethacrylate; Bis-MPEPP: 2,2-bis[4-(2-methacryloyloxyethoxy)phenyl] propane.

3.2.2. RESTORATIVE PROCEDURE

In this experiment, extracted human premolars were used according to protocol approved by the ethical institutional review board at Tokyo Medical and Dental University.

The coronal parts of 10 teeth were reduced by a low speed diamond saw (Isomet, Buehler, IL, USA) to obtain a flat occlusal dentin surface and then polished with 600-grit silicon carbide papers. Round class-I cavities 3 mm in diameter and 1.5 mm in depth were prepared in each specimen. After application of BF adhesive, the specimens were divided into two groups. First group was filled by incremental technique using ESQ universal composite. Second group was filled with flowable lining composite using PLV and bulk filling using ESQ composite (Figure-12).

Ten serial B-scan images were obtained throughout each cavity by a hand-held SS-OCT probe (Dental SS-OCT Prototype II, Panasonic Healthcare Co., Ltd, Ehime, Japan) for each specimen at a center wavelength of 1330 nm. Significant peaks in the signal intensity were detected at the bonded interface of the cavity floor and to compare the different filling techniques. The specimens were later cut into beams and tested to measure MTBS at the cavity floor.
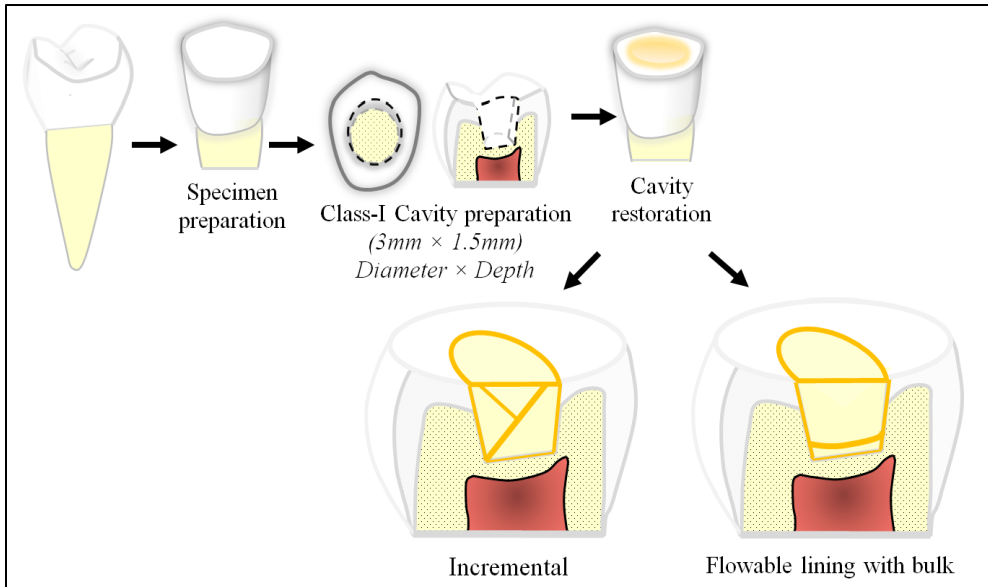
Figure-12:

Schematic drawing for the sample preparation for testing under the SS-OCT and MTBS. Each of the human premolars was subjected to trimming of occlusal surface (specimen preparation) and cavity preparation. Resin composite was applied using incremental and flowable lining with bulk filling techniques and according to the manufacturer instructions after application of the adhesive material.

3.2.3. OCT SYSTEM

Swept-source optical coherence tomography is a variant of OCT. SS-OCT time-encodes the wavenumber by rapidly turning the narrowband and source through a broad optical bandwidth (Table-4). Fringe response

versus frequency is detected with a balanced detector and the signal is Fourier transformed to obtain a depth-reflectivity profile from which a cross- sectional image is reconstructed. This prototype system is based on Swept Source Optical Coherence Tomography with a high-speed frequency swept external cavity laser as the light source at a center wave length of around 1330 nm with a waveband of over 100 nm and sweep rate of 30 kHz (Figure-13). The system can provide 2D and 3D images of the dental structure intra-orally, with lateral and axial optical resolution of 20 μm and 12 μm, respectively. The hand-held intraoral probe has been specifically designed for dental use. The intraoral probe is equipped with a CMOS camera that enables photographic visualization of the surface being scanned in real-time. The probe power is less than 10 mW, within the American National Standards Institute safety standard.

Figure-13:

Photographic image of the SS-OCT system. The sample arm is a hand-held scanning probe capable of scanning in 2D (x, z) and 3D (x, y, z) modes in maximum dimensions of 9 x 7 and 7 x 7 x 7 (mm), respectively. The probe is portable and designed for intraoral imaging.

Table-4: SS-OCT technical parameters and specifications.

Swept-Source OCT (Panasonic Healthcare Co., Ltd, Japan)	
Parameter	Specification
Wavelength	1330 nm ± 10 nm
Axial resolution	12 μm (in air)
Lateral resolution	20 μm (in air)
A-line rate	30,000 line/sec
2-D Frame A-scan Lines	2000 line / frame
Imaging depth	7 mm
Imaging width	9 mm
Image dimension (2D)	2000 x 1019 pixels
Low-power (<10 mW) Near-infrared Class 1 Laser	

3.2.4. ANALYSIS

A.   OCT DATA ANALYSIS

SS-OCT raw B-scan data were imported to an image analysis software (ImageJ ver. 1.42q) [32] to detect significant increase in the signal intensity at the resin-dentin interface at the cavity floor. The OCT data analyses were conducted as we described previously [3]. The higher

signal intensity appeared as bright clusters formed by bright pixels at the interface. In order to calculate the size of those bright clusters, an image analysis procedure was followed; the size scale was set, and the image was subjected to a median filter (1 px radius) to reduce the noise. The median filter is a non-linear digital filtering technique, often used to remove noise as a typical pre-processing and widely used step to improve the results of later processing. Median filtering is very in digital image processing because under certain conditions, it preserves edges while removing noise [3]. These steps were performed by a plug-in we compiled for the software. The image was then cropped to the area including the cavity floor in the center, of which the height was 500 μm (optical), and the width was equal to that of the cavity floor according to the location of the slice. The cropped image of the cavity floor was subjected to the binarization process according to the Isodata algorithm [3] in the auto-threshold function of the software to determine the target pixels with significantly higher brightness compared to other pixels in the background. Image binarization converts a grayscale image to a binary image (bi-level or black and white image), using a certain threshold (cut-off range) to visualize important information in an image. In an automated binarization process, the target image is produced base on a threshold determined

automatically using an algorithm. On the binary image, the length of each bright cluster along the cavity floor was calculated.

Bright cluster length percentage representing the non-bonded length (%) of the cavity floor on each cross-section was calculated according to the following equation:

Bright clusters length % = (total length of bright clusters at each slice)/ (length of the cavity floor at that slice) ×100

The number of slices, which showed no detectable brightness at the cavity floor, was also recorded for each composite material.
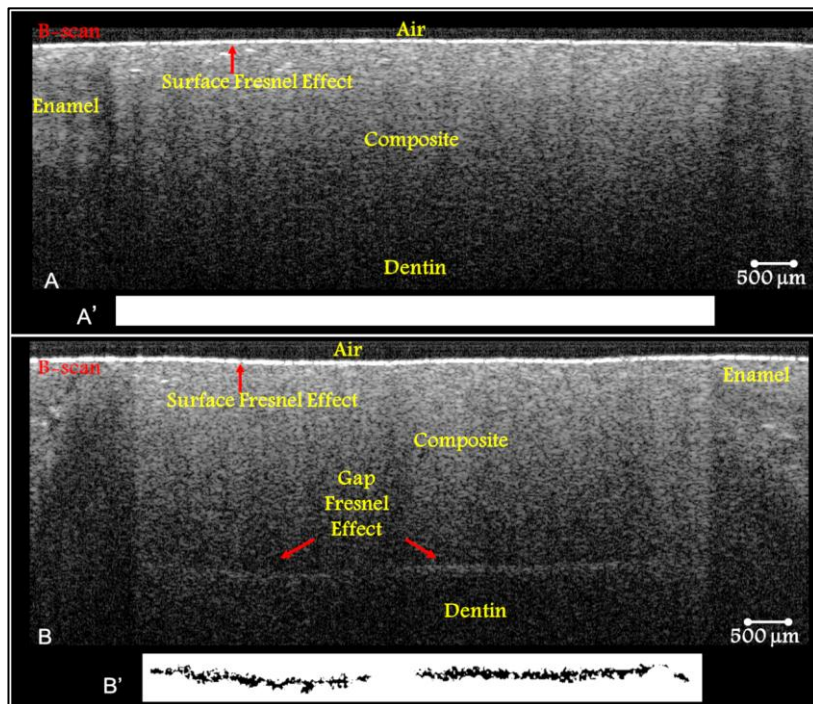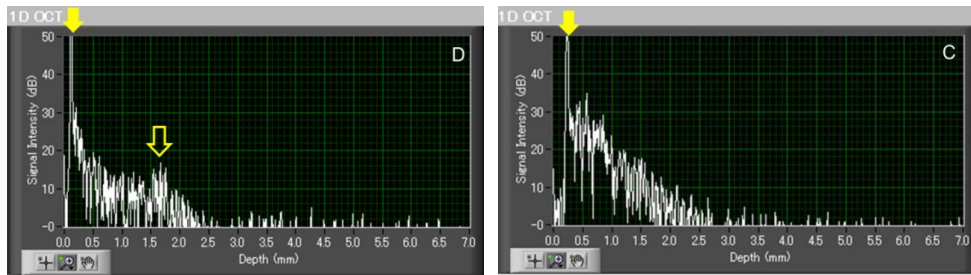
Figure-14:

Images obtained for restored class-I cavities with different filling techniques. (A) B-scan image for a cavity restored with BF bonding system and ESQ composite restoration using incremental filling technique. The cavity floor showed no increase in the signal intensity with no distinction between the composite resin and cavity floor. (B) B-scan of a cavity restored with PLV as a lining composite followed by bulk filling using ESQ composite. The interfacial area displayed an increase in signal intensity, which represented as white clusters or Fresnel reflection. (B`) is a binarized interfacial segment of (B). After applying the binarization process to the image reconstructed from the raw data, white clusters at interfacial region were converted to black pixels, and any other pixels were considered as the background. This explain the absence of black pixel in (A`). (C, D) SS-OCT signal intensity (A-scan) plotted against corrected depth for the lines in (A, B), respectively. The corrected depth was calculated by dividing the obtained depth from OCT image by the refractive index of the medium, which was 1.5 in this case. The solid arrows in (C &D) show reflection from the surface of the composite (interface with air) for both line profiles, while the blank arrow in (D) points to the second peak indicating reflection from an interfacial gap. Note that no detectable change in signal intensity is observed at those parts of the interface without gap as seen with incremental technique in (C).

B.   MTBS AND FRACTURE MODE ANALYSIS

After SS-OCT scanning, all specimens were processed for test of adhesion to the cavity floor by MTBS. For this purpose the cavities were serially sectioned using Isomet saw in two directions to obtain beams 0.7×0.7 mm in dimensions. The beams were in turn attached to a MTBS jig using cyanoacrylate glue and tested in a universal testing machine at a cross-head speed of 1 mm/min. For analysis of fracture mode after the MTBS test, representative debonded specimens were gold-coated and observed using a scanning electron microscope (SEM).

3.3. RESULTS

Typical B-scan images acquired by SS-OCT for each group were presented in Figures-14 (A, B). In figure-14A, unlike the incremental filling group, the B-scan image for lining filling technique (Figure-14B) showed bright clusters at the cavity floor, which represent gap at the bonded interface. Statistical analysis was performed by a *t*-test to find whether there was a significant difference between the groups using the two testing methods. The results indicated no significant difference in MTBS testing in both filling techniques as well as cavity adaption results by OCT ($p > 0.05$ for both methods), while the two methods exhibited a similar trend as seen in (Figure-15A). When the results

were pooled, Pearson correlation showed a significant but moderate correlation between the average MTBS value from each tooth and average adaptation (%) by OCT from the same tooth ($r = 0.674$, $p < 0.01$). High magnification images of the mode of failure in each filling group by SEM represent incremental filling technique (Figure-16A) which demonstrated a failure at the interface between BF bonding resin and dentin (adhesive failure), while lining filling technique in (Figure-16B) represents mixed failure including cohesive fracture in bonding, failure between adhesive and composite and failure at resin-dentin interface.

3.4. DISCUSSION

SS-OCT provides a cross sectional image with good resolution that permits instant non-invasive visualization of the underlying defects in a biological tissue or biomaterials. In comparison to the dye penetration test and ground sectioning techniques that require slicing and making the entire margin visible for examination, this study revealed the remarkable capability of the SS-OCT in detection and quantifying micrometer gaps under the composite restorations non-destructively.
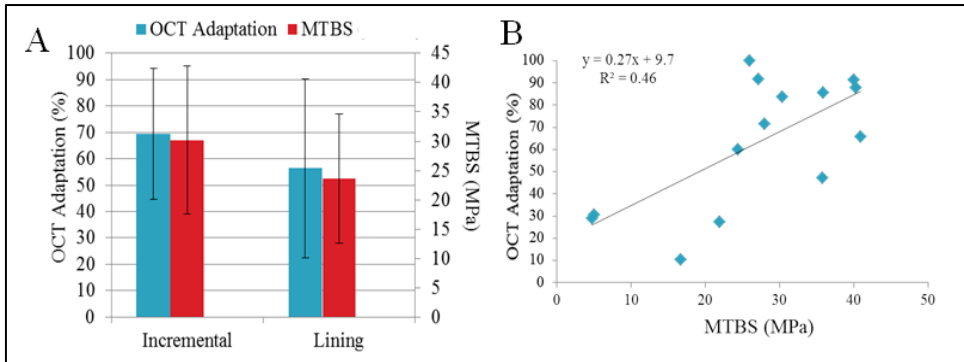
Figure-15:

Graphs representing relationship between OCT and MTBS measurements. (A) The adaptation of the bonded complex at the cavity floor (gap free cavity floor) and MTBS; in both groups, followed similar tendencies with no significant difference between filling techniques ($p > 0.05$). (B) The Pearson correlation was significant between the two variables ($r = 0.675$, $p < 0.01$).
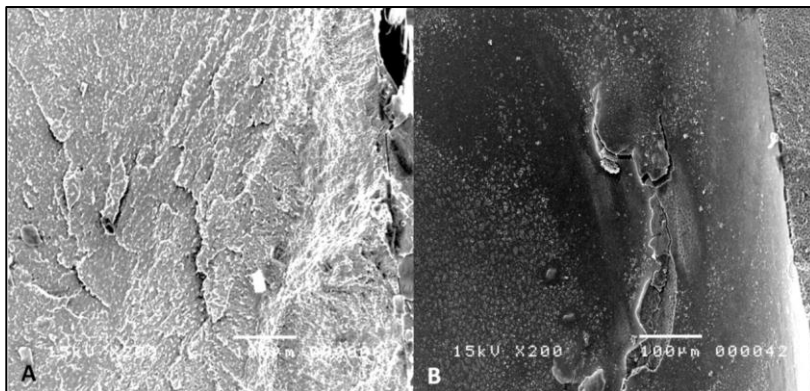
Figure-16:

High magnification images by SEM, which demonstrated the mode of failure in each filling group. (A) It represents incremental filling

technique which demonstrated a failure at the interface between BF bonding resin and dentin (adhesive failure). (B) The obtained image by SEM represents mixed failure including cohesive fracture in bonding, failure between adhesive and composite and failure at resin-dentin interface. Note that it would be difficult to locate the axial position of these failures under SS-OCT images, as under the current resolution the interfaces are indistinguishable especially in the case of thin adhesive layers (less than 10 μm thick).

In a previous study, we hypothesized that the alteration in the signal intensity (small peak) at the resin–dentin interface, which appeared as bright clusters; due to Fresnel phenomena, indicated loss of interfacial seal [3]. The refractive index of air, which we presumed was filling the gap, is 1.0 and that of teeth and composites are in the range of 1.5 - 1.6 [51]. Fresnel phenomena were clearly observed at the tooth or composite top surface, where the high-intensity light crossed air-substrate interface [26], as in figure-14A. In contrast, fading of the light wave as it pass through the resin and down to the dentin results in weaker signal intensity at the 1.5 mm of the composites depth. Although the signal intensity was low at that composite depth, the Fresnel reflection was clearly detected in some specimens at the interfacial areas (Figure-14B), when the light encountered a low refractive media during its passage from the resin to dentin. The

binarization image analysis method we employed could outline the areas with intensified backscatter signal intensity (or bright pixel clusters on the image). These clusters are variable in length and height at the interface, and in the extent of brightness too. In another report, it was demonstrated that the lengths of these bright clusters represented the extent of gaps, while their axial size was not necessarily the vertical size of the defect. This was thought to be due to the edge-depending nature of this method. It is noteworthy that apart from the defect edges, the non-scattering medium inside defect, presumably air, would appear dark (back ground noise signal intensity) in the SS-OCT image.

The dental SS-OCT system employed in this study is designed to obtain images of dental tissues intra-orally. However, further investigation is underway to confirm whether the image analysis methodology used in the laboratory test is adequate for clinical images. One important point to be considered here is that the depth and shape of the cavity in the laboratory settings are standardized considering the attributes of light penetration and reflection-based imaging and optical properties of the biomaterials and tissues involved. On the other hand, in a clinical practice, the cavity is prepared based on the shape and size requirements of each single case, and therefore quantitate assessment

may require a more sophisticated image analysis strategy. Nevertheless, immediate qualitative visualization of composite structure and margins, itself, is a highly desirable and attractive capability of this clinical imaging system.

This study measured the percentage of the bonded interface and the bond strength of the restored class-I cavities using two different filling techniques. The total adaptation (gap-free interface) percentage and bond strength results demonstrated a similar trend in each group. According to the obtained results, when the highly filled ESQ composite was used in conjugation with incremental filling technique, it showed slightly improved adaptation of the composite to the cavity floor, which might be related to the reduced amount of the placed composite increment (Figure-12) with reduced contraction stress [52]. Moreover, the high filler contents in this composite decreased volumetric polymerization shrinkage. On the other hands, PLV is a flowable composite with higher filler content and higher elastic modulus compared to conventional flowables; however it still showed higher shrinkage than universal and posterior composites, which may have generated stresses when placed as a base covering the whole adhesive-treated floor and lower parts of the cavity walls with a cavity

configuration (C-factor) equal to that of the class-I cavity. In this study, we could not confirm additional benefits of cavity lining using this composite, while further investigation is required to clarify the cause. Also, it has to be mentioned that an all-in-one adhesive system was selected in the present study, though it was indicated that the simplified adhesive showed substandard performance in comparison to the predecessor two-step self-etch adhesive [41].

3.5. CONCLUSION

Quantitative assessment of dental restorations by SS-OCT can provide additional information on the performance and effectiveness of dental composites and restoration techniques. Furthermore, results of the non-invasive interfacial gap assessment showed a similar trend to those obtained by MTBS. In addition to the laboratory testing, an OCT system equipped with an intraoral probe may become a useful clinical tool for the assessment of existing bonded composite restorations.

3.6. ACKNOLEDGMENT

CHAPTER 4: CONCURRENT EVALUATION OF COMPOSITE INTERNAL ADAPTATION AND BOND STRENGTH IN A CLASS-I CAVITY

CHAPTER 4

CONCURRENT EVALUATION OF COMPOSITE INTERNAL ADAPTATION AND BOND STRENGTH IN A CLASS-I CAVITY

4.1. INTRODUCTION AND OBJECTIVES

Polymerization shrinkage of the methacrylate-based resin composites upon curing is one of the major concerns in restorative dentistry [53-55]. The shrinkage upon free-radical polymerization of the resin may reduce up to 3% of the total composite volume, and generate contraction stresses [56, 57]. Generally, the contraction stresses depend on material composition, cavity configuration, volume of the material and the placement technique [58]. When the generated contraction stresses overcome the bond strength to the cavity walls, they will affect the marginal integrity, and result in the loss of the intermingling adhesion between the resin and dental structure. Moreover, the residual stresses may affect integrity of the restoration in the long-term; debonding at the cavity margins could potentially lead to

loss of the interfacial seal or microgap formation, microleakage, marginal staining, and bacterial invasion with secondary caries formation, pulp pathology and material degradation, and as a consequence, treatment failure [58, 59].

Several approaches have been taken by the manufactures to minimize polymerization shrinkage by incorporating more fillers and introducing new chemical resin formulations. Moreover, clinicians have also attempted to overcome the problem by applying thicker adhesives to the cavity walls to act as a stress absorbing layer, and implementing different filling techniques to improve the bond strength [60-62]. The effect of cavity configuration on the composite bond strength, when compared to flat surfaces, has been emphasized previously, highlighting the significance of contractions stress [63]. It has been suggested that by using an incremental filling technique, the reduced volume of the resin at each increment may decrease the contraction stresses at the tooth-restoration interface, and improve the bond strength. Alternatively, the application of a separately cured, low-viscosity resin between the adhesive system and the resin composite has been suggested as an approach to overcome contraction stresses and improve the bond strength [60, 61, 64-66]. However, none of these

techniques has become an established clinical standard based on adequate evidence, particularly for newly introduced materials such as the all-in-one adhesives.

The most common laboratory evaluation methods to investigate the effectiveness of composite restoration and the associated placement techniques have included restoration margin assessments and bond strength evaluations. The introduction of microtensile bond strength test (MTBS) has enabled the estimation of the local bond strength to a small area in bonded complex substrates [67-69]. While the MTBS methodology also allows preparation of samples from a filled cavity, the majority of research works on adhesion published using this method have dealt with flat surfaces, [70] perhaps due to the difficulty of preparing MTBS specimens from small cavities and controlling various relevant factors. It has been reported that MTBS testing on flat dentin surfaces may not predict the behavior of a material in the clinically relevant setups involving a cavity [71].

On the other hand, interfacial assessment of the restorations could be a valuable means to compare adhesives on a relative scale enabling inter-study comparisons. However, the commonly known in vitro microleakage tests, as conducted in the published literature, are

not reliable laboratory tests and valid predictors of the clinical outcomes [72]. The microleakage tests involving internal margins are both time-consuming and destructive, yet not universally established as a standardized methodology. Recently, there has been an increasing interest in technologies that can reconstruct images of the internal structures to study defects of resin composites, adhesion and shrinkage phenomena [34, 50]. Optical coherence tomography is an emerging technology, which demonstrated its utility in assessment and visualization of the cross-sections of the internal biological structures and some biomaterials at submicron scale non-invasively and non-destructively. It has been utilized to identify and quantify the interfacial gaps under the composite restoration without the need to cross-section the specimen [3, 34, 35, 73-75].

Several studies have investigated an association between adaptation and bond strength of dental composites; however, the relationship is not well understood [49, 70, 72, 76-78]. Non-destructive evaluation of cavity floor adaptation by OCT allows further processing of the same restoration for MTBS, and may help to elucidate such a relationship. Therefore, the objective of this study was to assess the cavity floor adaptation at the tooth-resin interface, and correlate the

findings with the MTBS of composites placed in class-I cavities following different filling techniques. The null hypotheses were that there was no relationship between cavity floor adaptation and bond strength, and that neither of the variables were affected by the filling technique.

4.2. MATERIALS AND METHODS

4.2.1. MATERIALS USED

The materials used in this study are listed in Table-5. The lot number and chemical composition of each material are according to the information provided by the manufacturers. Two all-in-one adhesive systems; Tokuyama Bond Force (BF; Tokuyama Dental, Tokyo, Japan) and Clearfil Tri-S Bond Plus (SE1; Kuraray Noritake Dental, Tokyo, Japan) were used in this experiment. Two composite resins in shade A2 were evaluated; Estelite Sigma Quick (ESQ; Tokuyama Dental), which is a light-cured universal composite resin with sub-micron spherical fillers, and Palfique Eselite LV (PLV; Tokuyama Dental) – medium flow type which is a low-viscosity, light-cured flowable composite with sub-micron spherical fillers.

Table-5: Adhesives system and composite resins used in this study.

Material (Manufacturer) (Code)	Composition	Lot No.	Fillers (%)
Tokuyama Bond Force (One-step self-etch adhesive) **(Tokuyama Dental, Japan) (BF)** **pH=2.3**	• 3D-SR • HEMA • Bis-GMA • TEGDMA • Glass fillers • Photoinitiators • Isopropyl alcohol • Water	139M	-
Tri-S Bond Plus (SE One-Japan) (One-step self-etch Adhesive) **(Kuraray Noritake Dental, Japan) (SE1)** **pH: 2.3**	• 10- MDP • Bis-GMA • HEMA • Hydrophilic aliphatic dimethacrylate • Hydrophobic aliphatic methacrylate • Colloidal silica • Sodium fluoride • Photoinitiators • Accelerators • Initiators • Ethanol • Water • Others	007A	-
Estelite ∑ Quick Universal Composite **(Tokuyama Dental, Japan) (ESQ)**	• Bis-GMA • TEGDMA • Silica–zirconia fillers • Silica–titania fillers • Photoinitiators	J018	82% weight (71% volume)
Palfique Estelite LV Medium-Flow Flowable Composite **(Tokuyama Dental, Japan) (PLV)**	• Bis-MPEPP • UDMA • Bis-GMA • TEGDMA • Silica–zirconia fillers • Silica–titania fillers • Photoinitiators	252	68% weight (49 % volume)

Abbreviations: 3D-SR: Methacryloyloxyalkyl acid phosphate, HEMA: 2-hydroxyethyl methacrylate; Bis-GMA: Bisphenol-A-diglycidyl methacrylate; TEGDMA: Triethyleneglycol dimethacrylate; 10-MDP: 10-methacryloyloxydecyl dihydrogen phosphate. UDMA: Urethane dimethacrylate; Bis-MPEPP: 2,2-bis[4-(2-methacryloyloxyethoxy)phenyl] propane.

4.2.2. RESTORATIVE PROCEDURES

The experimental design of this study and the use of thirty caries-free extracted human teeth were subjected to the guideline of the Ethics Committee of Tokyo Medical and Dental University, in accordance with the principles of the Declaration of Helsinki.

After cleaning with a dental scaler and removing the roots of the teeth, the occlusal cusps were grounded to obtain a flat occlusal table in enamel using a model trimmer. A standard cylindrical class-I cavity with the floor located in dentin, 3 mm in diameter and 1.5 mm in depth was prepared using a flat-end tapered cylinder diamond bur (ISO #021, Shofu, Kyoto, Japan) and finished with superfine flat-end diamond bur (ISO #013, Shofu) mounted on an air turbine headpiece (Ti-Max X, NSK, Kanuma, Japan), operated under copious cooling water. The bur was replaced after five preparations in order to maintain the cutting efficiency. The specimens were divided into two groups following the adhesive materials used; BF and SE1, which were applied and cured using a halogen light curing unit (Optilux 501, Kerr, CA, USA; 500 mW/cm^2 intensity), according to the manufacturers' instructions. Each group was then subdivided into 3 subgroups according to the filling technique; bulk (BUK), incremental (INC) and flowable lining followed

by bulk (LIN), with 5 teeth in each subgroup. In BUK, the universal composite resin was placed in a bulk; in INC, the composite was placed in 3 oblique increments, and LIN technique was done using the flowable composite as a thin liner (200 – 300 μm in thickness) followed by a single increment of the universal composite. Each composite layer was separately cured with the same curing unit and according to the manufacturer's instructions. A schematic drawing for the sample preparation and visualization under the OCT is shown in Figure-17.

4.2.3. SWEPT-SOURCE (SS) OCT SYSTEM

The OCT system (OCT-2000, Santec, Komaki, Japan) used in this study had the same setup components as described previously [3, 9]. The light source in this system sweeps the wavelength from 1260 nm to 1360 nm at 20 kHz sweeping rate with central wavelength at 1319 nm. The axial resolution of this OCT system is 11 μm in air, which corresponds to approximately 7 μm within a biomedical structure with a refractive index of around 1.5. The lateral resolution of 37 μm is determined by the objective lens and beam diameter inside the probe. The focused light-source beam is projected onto the sample and scans across the area of interest in two dimensions (x, z) using a hand-held probe. Backscattered light from the sample is returned to the system,

digitized in time scale and then analyzed in the Fourier domain to reveal the depth-resolved reflectivity profile (A-scan) at each point.

The combination of a series of A-scans along the section of interest creates a raw data file (B-scan) with information on the signal intensity (backscattered light) and x, z coordinates from each point within the scanned area. Two-dimensional cross-sectional images can be created by converting the B-scan raw data into a gray-scale image [3, 26].

4.2.4. TOMOGRAPHIC IMAGING

After storing the restored specimens in a humid state at the room temperature for 24 hours, each specimen was fixed on a micrometer head stage and subjected for tomographic imaging by OCT. The scanning probe with scanning beam was projected perpendicular toward the occlusal surface. Ten serial B-scans were obtained along the restoration at 250 μm interval distance, which was accomplished in bucco-lingual cross-sections [9]. A significant increase in the signal intensity at the resin-dentin interface at the cavity floor indicated a gap. The length of these gaps was calculated at the cavity floor on each B-scan image using a digital software (ImageJ ver. 1.45q, National Institutes of Health, MD, USA) as described previously [3, 9, 34]. The

adaptation parameter was defined as adaptation % = [(total cavity floor length – sum of gap length) / total cavity floor length] x 100.

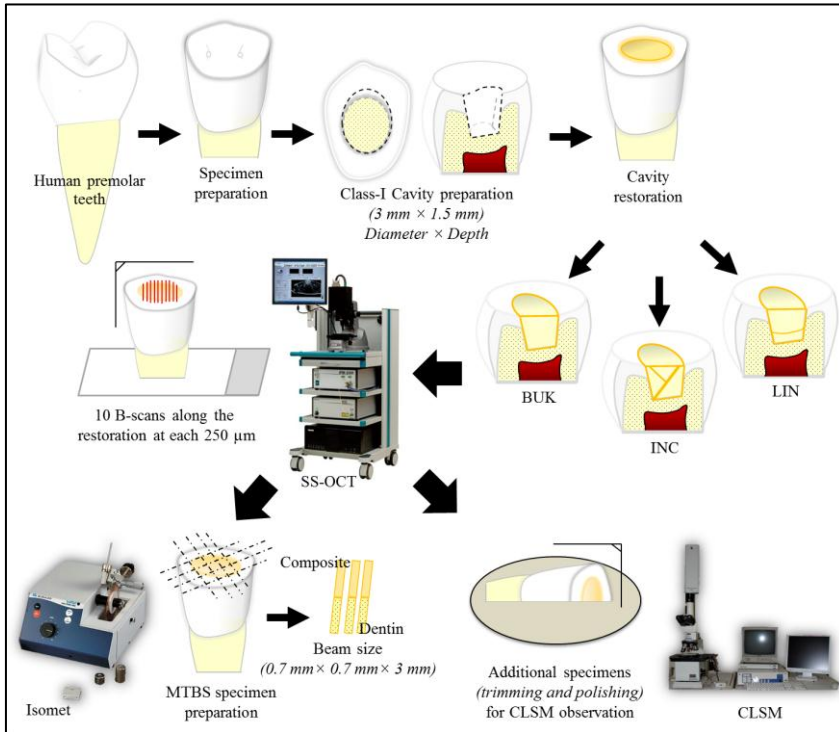**Figure-17:**

Schematic diagram showing the study design and methodology. After application of the adhesive material, cavity restoration was completed using composite restoration in BUK, INC or LIN techniques. Ten serial B-scans were obtained for each specimen by OCT; the specimens were later sectioned for MTBS testing. Additional specimens were prepared and restored for CLSM observation.

4.2.5. MTBS SPECIMEN PREPARATION AND MEASUREMENT

After tomographic imaging, the specimens were sectioned using a slow-speed diamond saw (Isomet, Buehler, IL, USA) under water coolant to produce parallelepiped sticks (0.7 × 0.7 × 3 mm) with their long axis perpendicular to the cavity floor. The ends of the sticks were carefully glued to a testing jig using cyanoacrylate glue (Zapit, Dental Venture of America, CA, USA), in a tabletop testing machine (EZ Test, Shimadzu, Kyoto, Japan) and subjected to a tensile force at a crosshead speed of 1 mm/min. The actual cross-sectional area of each stick was measured using a digital caliper (CD15, Mitutoyo, Kawasaki, Japan). Then, MTBS values to the cavity floor were calculated in MPa by dividing the fracture load by the surface area, measured to the nearest 0.01 mm with the digital calipers. Every cavity was expected to produce 9 beams; in case a beam failed prior to MTBS testing (pre-test failure), a value of zero MPa was recorded. For analysis of fracture mode after the MTBS test, representative de-bonded specimens were gold-coated and observed using a scanning electron microscope (SEM, JEOL, Tokyo, Japan). Fracture mode of each beam was classified as one of the following patterns: cohesive failure through resin (CR); failure exclusively at the joint between bonding resin and composite (BC);

mixed failure including composite, adhesive and dentin (MX); failure between bonding resin and dentin (AD); cohesive failure in dentin (CD).

4.2.6. CONFOCAL LASER SCANNING MICROSCOPE (CLSM) OBSERVATION

Twelve additional samples were prepared for the confirmatory cross-sectional examination under CLSM (1LM21H/W, Lasertec, Yokohama, Japan). The specimens were subjected to OCT imaging. In order to perform interfacial imaging, the specimen was reduced up to the cross-section that was previously imaged by OCT using different sizes of silicon carbide papers (280 ~ 2000) grit in an ascending direction. Finally, the specimens were additionally polished with diamond paste down to a particle size of 0.25 μm in circular motion under copious cooling water, and subjected to CLSM imaging at (1250×) magnification.

4.2.7. STATISTICAL ANALYSIS

Since the distribution of data in each group was normal (Kolmogorov Smirnov $p > 0.05$), parametric tests were performed. The OCT cavity floor adaptation and MTBS were analyzed using two-way ANOVA to test the effect of adhesive material, filling technique, and their interactions. For pairwise comparisons among the filling techniques using each adhesive material and between the adhesives under the

same filling technique, independent Student's *t*-tests were used with Bonferroni correction of the significance level. The relationship between OCT cavity floor adaptations and MTBS was investigated by a Pearson's correlation followed by a linear regression. All of the statistical analyses were performed using the Statistical Package for Social Science (SPSS for Windows, Version 16.0, SPSS, IL, USA) with the significance level defined as alpha = 0.05.

4.3. RESULTS

The obtained results in this study are presented in figures (18-20). The OCT images of some cavities showed increased signal intensity in the form of bright clusters at the cavity floor, which represented a gap at the bonded interface. Moreover, the internal defects such as voids or trapped air were clearly observed. The increased signal intensities (white clusters) in B-scans at the bottom of the composite restoration corresponded to the gap in confirmatory CLSM images (Figure-18 and Figure-19). On the other hand, the area that did not demonstrate an increased signal intensity demarcating the interface at the cavity floor showed a good adaptation between the bonded dentin-resin complex in CLSM images (Figure-20).

The independent factors adhesive systems ($p < 0.05$), filling techniques ($p < 0.05$) as well as their interaction ($p < 0.05$) presented significant difference among the tested groups in the MTBS. For adaptation, although the adhesive system was not a significant factor ($p = 0.478$), filling techniques and their interaction with materials were significant ($p < 0.005$). Pairwise comparison of cavity adaptation between different filling techniques did not present a significant difference within BF ($p > 0.05$), while in SE1, BUK technique was significantly different from other techniques ($p < 0.05$) (Figure-21a). On the other hand, MTBS revealed a significant difference between BUK and INC filling techniques in BF ($p < 0.05$). Similarly, in SE1, BUK technique showed a lower mean value that was significantly different from other techniques ($p < 0.05$). In comparison of MTBS between the two adhesives, SE1 mean values in LIN were significantly greater than those of BF under the same technique (Figure-21b). In general, OCT comparisons revealed that INC had the highest mean adaptation values, which corresponded to the result obtained by MTBS test.

Figure-18:

B-scans and CLSM images obtained for the restored BUK group specimens. Blank arrows on OCT images point to the same area observed under CLSM. (a) In BF-BUK group, as the light traversed from the composite toward the dentin, a high signal intensity area was detected at the bonded interface. (a') A binary image after applying the binarization process to the cropped interfacial area. (a") The interfacial gaps location in the cross-sectional images, which obtained by the CLSM were correlated with the bright area location in (a) and target pixels in (a'). (b-b") Similar phenomena were detected in SE1-BUK technique. Unlike (a"), the detachment in (b") appears to have occurred at the resin-dentin interface.
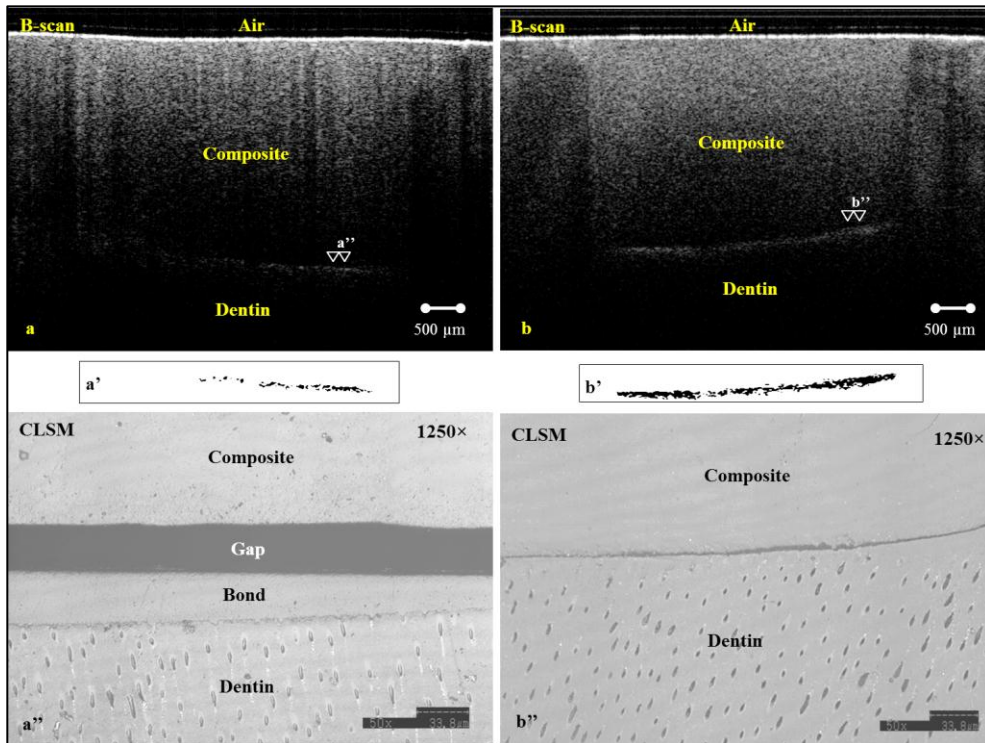
92

Figure-19:

B-scans and CLSM images obtained for the restored LIN group specimens. Blank arrows on OCT images point to the area observed under CLSM. (a-a") In BF-LIN, the existence of white clusters in B-scans (a), was correlated with binarized image of the selected interface (a'), and the actual gap was observed in the confirmatory CLSM images (a"). (b-b") Similar gaps were detected in SE1-LIN application method as well.

According to the correlation analysis, a significant and positive relationship was found between the two parameters; the cavity floor adaptation (%) obtained from B-scans and the mean MTBS (MPa) for each specimen (Pearson correlation coefficient r = 0.72 with 95%

confidence interval of 0.49 to 0.89, p < 0.001), accompanied with a significant linear regression (R^2 = 0.52, p < 0.001) (Figure-21c).

The modes of failure of the tested groups are summarized in Figure-22 together with representative high magnification images of the fracture mode patterns. The failure modes were remarkably different among BF groups; CR was predominant in BF-BUK, while MX was the most frequent in BF-INC. A large number of samples showed BC failure in BF-LIN. On the other hand, most of the failures in SE1 groups were AD.
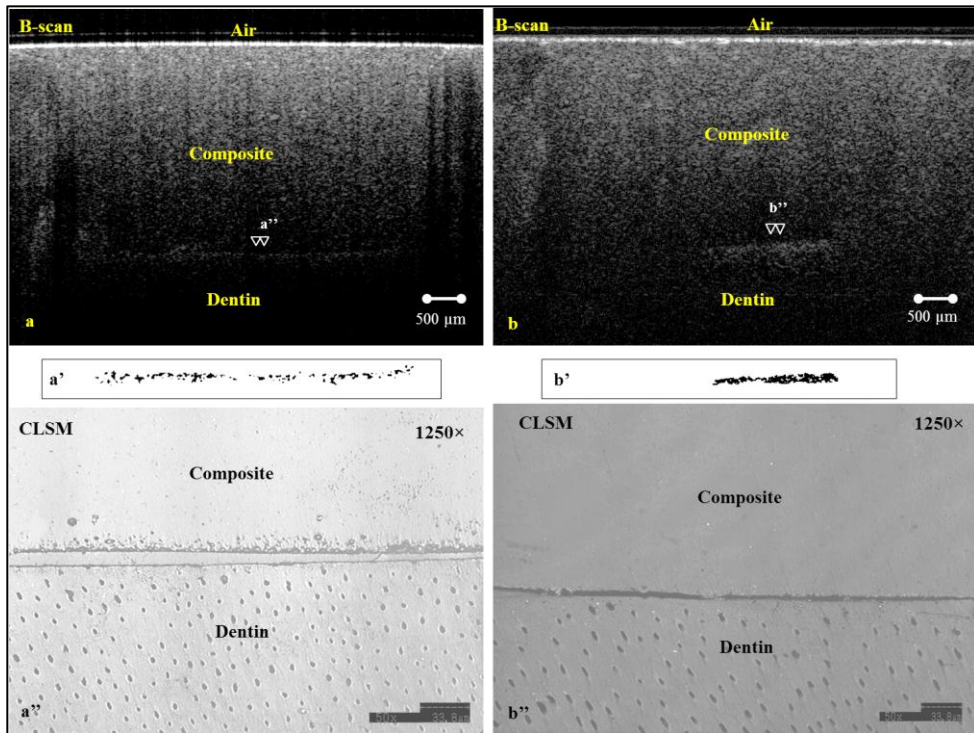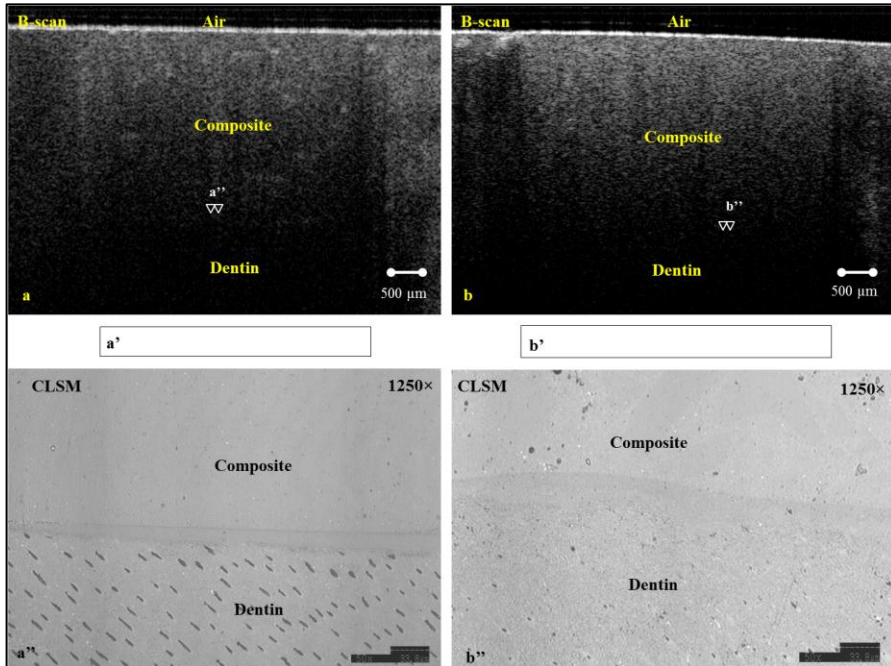
Figure-20:

B-scans and CLSM images obtained for the restored INC group specimens. Blank arrows on OCT images point to the area observed under CLSM. (a) The coherent laser beam in B-scan for BF-INC did not encounter any sudden change in the refractive indices (significant scattering) while passing through the bonded complex. Therefore, it was difficult to demarcate the interface from the surrounding substrate on the resulting B-scan. (a') A binary image for the cropped interfacial area. Image processing did not detect any bright area at the interface which did not represent any target pixels. (a") Examination under high magnification of the obtained CLSM images revealed the intimate adhesion between composite-adhesive-dentin substrates. (b-b") Similar outcome were seen in SE1-INC subgroup.
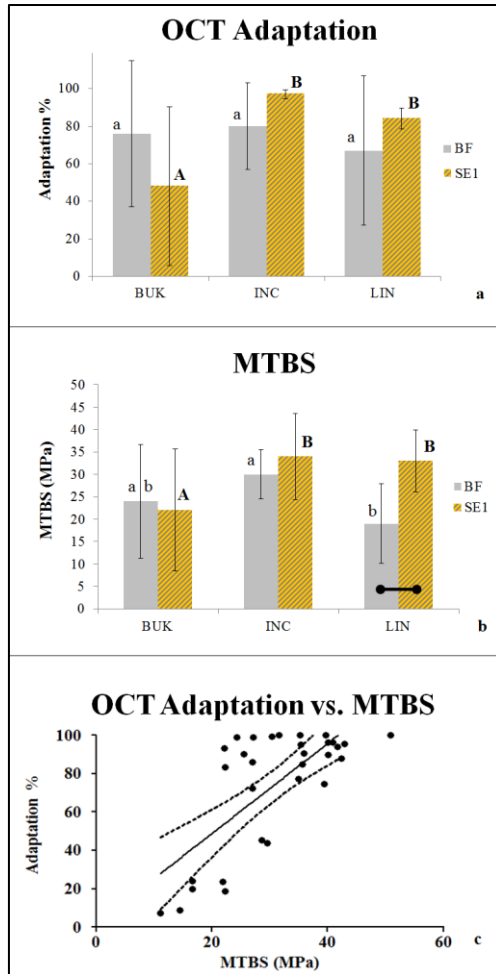
Figure-21:

(a) A graph indicating the cavity floor adaptation percentage, (b) MTBS of various tested groups. Groups marked with the same lowercase letter with the same material are not significantly different (p > 0.05). Horizontal bar indicates significant difference between the materials under each technique (p < 0.05). (c) Regression line between cavity floor adaptation and MTBS (y = 2.3x + 1.8, R^2 = 0.52, p < 0.001). The dotted lines represent 95% confidence interval of the regression.

4.4. DISCUSSION

SS-OCT is one of the latest implementation of OCT imaging technology that provides cross- sectional images with higher resolution and speed compared to the conventional time-domain systems, permitting instant imaging of the underlying defects in a biomaterial. In comparison to the dye penetration test and ground sectioning techniques that require slicing and making the entire margin visible for examination, OCT has the remarkable capability of quantifying micrometer gaps under the composite restorations non-destructively [3, 9, 34]. This should allow a comprehensive assessment of the whole cavity adaptation, without the complications arising from the physical sectioning methods.

Generally, the imaging depth of OCT systems has been reported to be in the range of 2-3 mm [3, 26], depending on the optical attenuation parameters within the substrate being imaged. In this study, the OCT was operated to examine the dentin cavity floor for the presence of gaps with different filling techniques and different types of adhesive restorations, in cavities only 1.5 mm in depth, to ensure adequate signal discrimination at the interfacial defects [3]. In previous studies, it was confirmed that a significant increase in the signal intensity (peak) at the tooth-restoration interfacial zone, which

appeared as bright clusters, indicated loss of interfacial seal [34, 35], and the horizontal dimension of the bright cluster at the cavity floor strongly correlated with the actual extension of the gap measured by CLSM on the same cross-sections [9]. The signal intensity peak at the defect boundary was attributed to the Fresnel reflections or diffuse reflections of light when passing through media with differing refractive indices; the refractive index of air, which we presumed was filling the gap, is 1.0 and that of water is 1.33, while those of teeth and composites are in the range of 1.5 - 1.6 [79]. In addition to the defect boundaries, this phenomena is evidently observed at the air-tooth, air-composite external boundary, where the high-intensity light traversed the air-substrate interface [27].
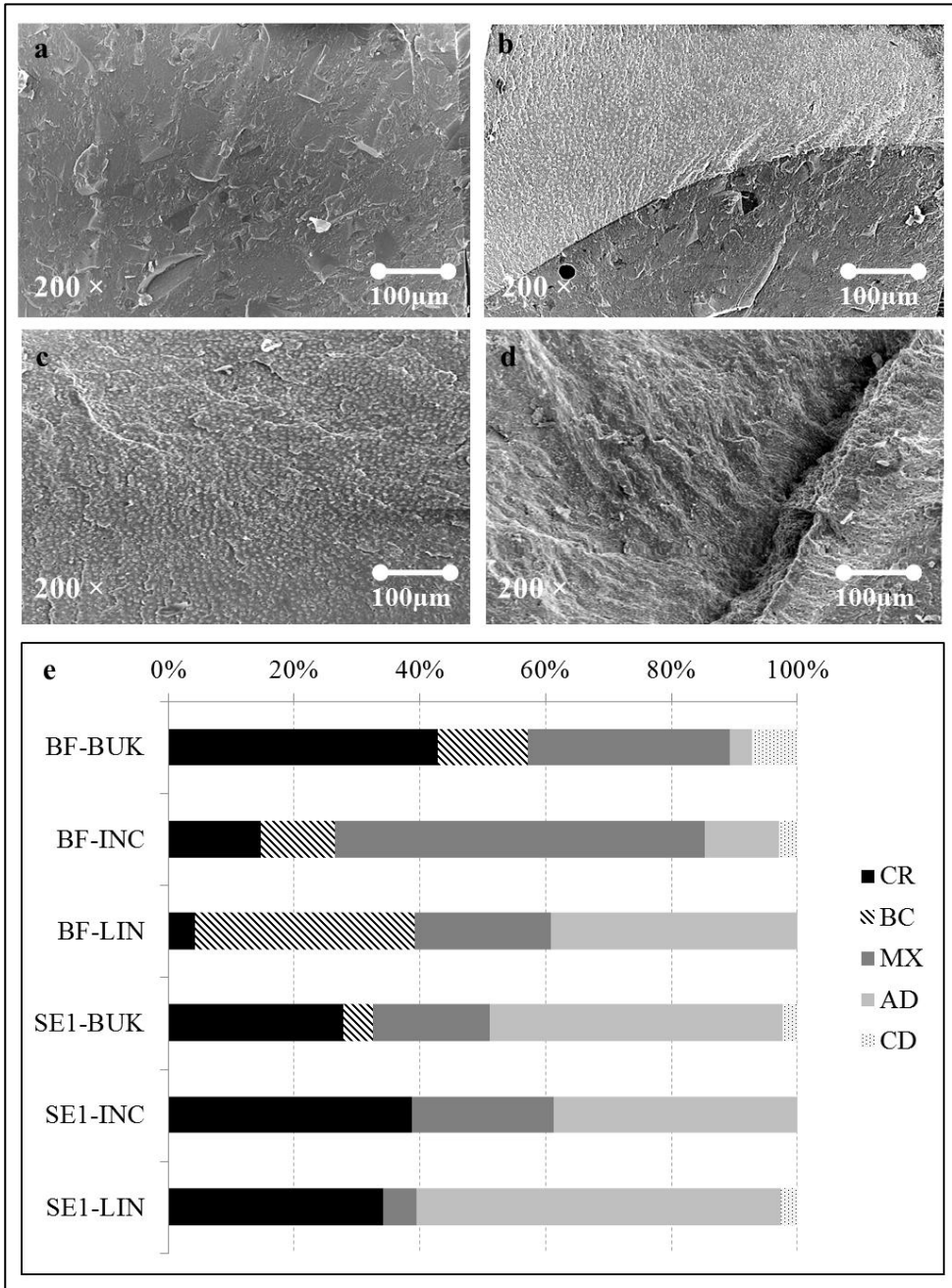
Figure-22:

(a-d) Representative SEM images to illustrate the fracture pattern. (a) Cohesive failure in resin (CR); (b) Mixed failure partially including

composite (MX), adhesive and dentin; (c) Failure between adhesive resin and dentin (AD); (d) Cohesive failure in dentin (CD). (e) A summary of mode of failures results of the tested groups. BF: Tokuyama Bond Force; SE1: Clearfil Tri-S Bond Plus; BUK: Bulk technique; INC: Incremental technique; LIN: Flowable lining with bulk filling. Failure between composite and bonding agent (BC).

Longitudinal clinical trials have a great scientific impact on determining the efficiency of restorative materials. On the other hand, they are time consuming and require a large sample size, which is difficult to be uniform and standardized. Therefore, laboratory studies simulating the clinical condition are essential as an alternative prospect. Bond strength test in a cavity setup may be essentially different from the flat surface that is commonly used as the bonding substrate for the laboratory research. In this regard, in addition to those differences associated with C-factor, bonding layer thickness may be significantly affected by the shape and the presence of line angles in a cavity as opposed to a free flat surface [80]. Moreover, evaporation of water and solvents from adhesive in the cavity is affected by air-drying, which in contrast to the flat surface may be influenced by the cavity depth and shape [41, 80].

In this study, the relationship between cavity floor adaptation with different filling techniques and average MTBS obtained from the same cavities was evaluated. A moderate correlation was found between the two variables, indicating the validity of this OCT methodology for an overall comparison among restoratives and techniques to fill in a cavity. It should be noted that the nature of the two variables is different, and therefore, the parameters of this regression are likely to be affected by different factors. In this regard, bond strength is a fracture strength value, which not only depends on the adhesiveness of the bonding agent, but also is affected by the mechanical properties of the components (tooth, bonding resin and composite). On the other hand, OCT cavity floor adaptation is solely quantifying the sealed restoration interface. As observed in the regression plot of the pooled data (Figure-21c), in the cavities where high bond strength (> 40 MPa) was observed, there was no specimen showing a remarkably low adaptation. On the other hand, at lower bond strength values adaptation results were more variable. The relationship between these two variables was affected by the pretest failures; in other words, specimens prepared from areas where an interfacial gap had occurred, predominantly failed prior to the test and were recorded as null bond strength. Moreover, strong contraction

stress generated within the bulk of composite upon curing in high-modulus (low relaxation) materials could lead to initiation of micro-cracks within the material [81]. These defects may propagate during MTBS preparation and affect ultimate strength of the material, [82] which will in turn result in low MTBS.

According to the results, the filling technique appeared to be a significant factor affecting adaptation while the bonding system did not. Estimated marginal means for both adhesives indicated that the usage of the universal composite in conjugation with INC filling technique improved the adaptation and MTBS of the composite to the cavity floor. This finding might be related to the reduced volume and C-factor of each increment, which in turn reduced the polymerization shrinkage and the generated contraction stresses. According to the pairwise comparisons among SE1 groups, BUK technique showed the lowest mean, while INC and LIN demonstrated significantly improved cavity floor adaptation and MTBS. For BF, the INC showed highest MTBS, which was significantly higher than LIN. These results are in agreement with previously reported studies on the advantages of INC filling [64, 65].

Another finding of interest in the results of this experiment was the difference in MTBS between BF and SE1 under LIN technique, and highly variable adaptation of BF-LIN group. Some studies have reported incomplete removal of the solvent from the surface of all-in-one adhesives upon polymerization [83], which will hamper effective copolymerization between the composite and adhesive resin, [84] especially if the composite is not placed under adequate pressure to break the barrier of solvent/low-reactive monomers. Both adhesives; SE1 and BF, comprise the hydrophilic monomer HEMA, but utilize different organic solvents (SE1: ethanol, BF: isopropyl alcohol). Isopropyl alcohol has relatively a lower vapor pressure (4.1 kPa at 20°C) than ethanol (5.8 kPa at 20°C), which means that it requires more time to evaporate during air-drying phase [84]. The speculation gains support from the CLSM and SEM images of the interface in BF, showing frequently small voids or "bubble-like" areas at the flowable composite and adhesive resin interface (Figure-23). Interestingly, frequent failure between composite and bonding agent (BC mode) in BF-LIN group confirms the role this important joint in adhesion. It is suggested that although the use of a flowable composite as a liner can reduce stress generated by polymerization shrinkage in a high C-factor cavity, the incondensable composite may not provide adequate displacement

pressure to the residual solvent at the bonded interface of some adhesives; which was not seen with conventional composite placed incrementally.

Within the limitations of the research, which includes a narrow study design within a short period of time and limited number of tested materials, the proposed null hypotheses were rejected, as there was no relationship between cavity floor adaptation and bond strength, and neither of them were affected by the filling technique.
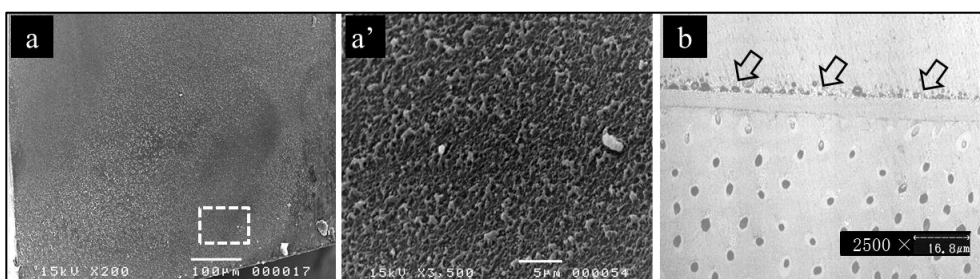
Figure-23:

SEM and CLSM images of BF-LIN subgroup. (a), (a') are SEM images of a fractured MTBS specimen that exhibited a failure at composite-adhesive interface (BC failure mode). At higher magnification (a'), small voids or "bubble-like" areas within the adhesive were detected. (b) High magnification CLSM image of a specimen in the same subgroup. The composite-adhesive interface appears to be unsealed, with several voids clearly observed at this interface (blank arrows).

4.5. CONCLUSIONS

OCT was utilized to determine the percentage of the debonded interface in a restored cavity non-destructively. There was a moderate correlation between floor adaptation and bond strength in class-I cavities. Overall, the placement technique of a universal composite affected adhesion in a class-I cavity, and the incremental technique showed the greatest potential.

4.6. ACKNOWLEDGEMENTS

CHAPTER 5

CHAPTER 5

GENERAL CONCLUSIONS

All of the studies included were limited laboratory experiments. Nonetheless, the potential for OCT-based diagnostics in the oral cavity is excellent. The penetration depth of this modality is adequate for most dental applications.

Based on the data available and the obtained results from the presented studies, a number of factors influencing the adaptation of resin-tooth inter-diffusion zone were identified and discussed.

- In chapter 1, SS-OCT imaging technology demonstrated a remarkable capability with high sensitivity and accuracy in detection and quantification of few micrometers gaps at the bottom of composite restorations, bearing the potential to become a clinical monitoring and a useful research tool in this field. Adaptation of composites to the cavity floor depended on multiple factors and not only on the polymerization shrinkage of composites or their filler contents.

- Chapter 2 concluded that quantitative assessment of dental restorations by SS-OCT can provide additional information on the performance and effectiveness of dental composites and restoration techniques. Furthermore, results of the non-invasive interfacial gap assessment showed a similar trend to those obtained by MTBS. In addition to the laboratory testing, an OCT system equipped with an intraoral probe may become a useful clinical tool for the assessment of existing bonded composite restorations.

- Chapter 3 showed that there was a moderate correlation between floor adaptation and bond strength in class-I cavities. For nanocomposite, an improvement in physical properties is expected due to the increased interfacial interactions between resin and fillers. Overall, the placement technique of a universal composite affected adhesion in a class-I cavity, and the incremental technique showed the greatest potential.

This work will have an important role in the laboratory and clinical evaluation of the success of the restoration. The results would lead to obtain clinical satisfaction by aiding the dentist in proper selection of

the restoration material and approaching gap free filling technique as well as identifying the actual cause of restoration failure.

Finally, this non-invasive imaging technique has a great potential for improving diagnostic and educational capabilities in oral cavity for applications ranging from teeth decay, through periodontal diseases to oral malignancy.

BIBLIOGRAPHY

BIBLIOGRAPHY

[1] Huang D, Swanson EA, Lin CP, Schuman JS, Stinson WG, Chang W, et al. Optical coherence tomography. Science. 1991;254:1178-81.

[2] Fujimoto JG, Brezinski ME, Tearney GJ, Boppart SA, Bouma B, Hee MR, et al. Optical biopsy and imaging using optical coherence tomography. Nat Med. 1995;1:970-2.

[3] Bakhsh TA, Sadr A, Shimada Y, Tagami J, Sumi Y. Non-invasive quantification of resin-dentin interfacial gaps using optical coherence tomography: validation against confocal microscopy. Dent Mater. 2011;27:915-25.

[4] Chinn S, Swanson E, Fujimoto J. Optical coherence tomography using a frequency-tunable optical source. Optics Letters. 1997;22:340-2.

[5] W. D, J. F. Optical Coherence Tomography; Technology and Applications. Berlin: Springer; 2008.

[6] T R, H H, E S. Art and Science of Operative Dentistry. Fifth Ed ed. India: Mosby; 2006.

[7] R M-P, A L. Nanotechnology: A Crash Course. USA: SPIE; 2010.

[8] Bakhsh TA, Sadr A, Shimada Y, Mandurah MM, Hariri I, Alsayed EZ, et al. Concurrent evaluation of composite internal adaptation and bond strength in a class-I cavity. J Dent. 2012.

[9] Bakhsh TA, Sadr A, Shimada Y, Khunkar S, Tagami J, Sumi Y. Relationship between non-destructive OCT evaluation of resins composites and bond strength in a cavity. In: Rechmann P, Fried D, editors. Proc SPIE 8208. 8 ed. San Francisco, California, USA: SPIE Photonic West, Lasers in Dentistry XVIII; 2012.

[10] Rigsby DF, Retief DH, Russell CM, Denys FR. Marginal leakage and marginal gap dimensions of three dentinal bonding systems. Am J Dent. 1990;3:289-94.

[11] Uyama S, Irokawa A, Iwasa M, Tonegawa M, Shibuya Y, Tsubota K, et al. Influence of irradiation time on volumetric shrinkage and flexural properties of flowable resins. Dent Mater J. 2007;26:892-7.

[12] Lee HL, Orlowski JA. Differences in the physical properties of composite dental restoratives. Suggested causes and clinical effects. J Oral Rehabil. 1977;4:227-36.

[13] Van Ende A, De Munck J, Mine A, Lambrechts P, Van Meerbeek B. Does a low-shrinking composite induce less stress at the adhesive interface? Dent Mater. 2010;26:215-22.

[14] Pashley EL, Agee KA, Pashley DH, Tay FR. Effects of one versus two applications of an unfilled, all-in-one adhesive on dentine bonding. J Dent. 2002;30:83-90.

[15] Wei S, Shimada Y, Sadr A, Tagami J. Effect of Double-application of Three Single-step Self-etch Adhesives on Dentin Bonding and Mechanical Properties of Resin-dentin Area. Operative Dentistry. 2009;34:716-24.

[16] Kakaboura A, Rahiotis C, Watts D, Silikas N, Eliades G. 3D-marginal adaptation versus setting shrinkage in light-cured microhybrid resin composites. Dent Mater. 2007;23:272-8.

[17] Sun J, Eidelman N, Lin-Gibson S. 3D mapping of polymerization shrinkage using X-ray micro-computed tomography to predict microleakage. Dent Mater. 2009;25:314-20.

[18] Haak R, Wicht MJ, Hellmich M, Noack MJ. Detection of marginal defects of composite restorations with conventional and digital radiographs. Eur J Oral Sci. 2002;110:282-6.

[19] Sun J, Fang R, Lin N, Eidelman N, Lin-Gibson S. Nondestructive quantification of leakage at the tooth-composite interface and its correlation with material performance parameters. Biomaterials. 2009;30:4457-62.

[20] De Santis R, Mollica F, Prisco D, Rengo S, Ambrosio L, Nicolais L. A 3D analysis of mechanically stressed dentin-adhesive-composite interfaces using X-ray micro-CT. Biomaterials. 2005;26:257-70.

[21] Levitz D, Hinds MT, Ardeshiri A, Hanson SR, Jacques SL. Non-destructive label-free monitoring of collagen gel remodeling using optical coherence tomography. Biomaterials.31:8210-7.

[22] Fercher AF, Mengedoht K, Werner W. Eye-length measurement by interferometry with partially coherent light. Opt Lett. 1988;13:186-8.

[23] Colston B, Sathyam U, Dasilva L, Everett M, Stroeve P, Otis L. Dental OCT. Opt Express. 1998;3:230-8.

[24] Colston BW, Jr., Everett MJ, Da Silva LB, Otis LL, Stroeve P, Nathel H. Imaging of hard- and soft-tissue structure in the oral cavity by optical coherence tomography. Appl Opt. 1998;37:3582-5.

[25] Feldchtein F, Gelikonov V, Iksanov R, Gelikonov G, Kuranov R, Sergeev A, et al. In vivo OCT imaging of hard and soft tissue of the oral cavity. Opt Express. 1998;3:239-50.

[26] Shimada Y, Sadr A, Burrow MF, Tagami J, Ozawa N, Sumi Y. Validation of swept-source optical coherence tomography (SS-OCT) for the diagnosis of occlusal caries. J Dent. 2010.

[27] Fried D, Xie J, Shafi S, Featherstone JD, Breunig TM, Le C. Imaging caries lesions and lesion progression with polarization sensitive optical coherence tomography. J Biomed Opt. 2002;7:618-27.

[28] Choma M, Sarunic M, Yang C, Izatt J. Sensitivity advantage of swept source and Fourier domain optical coherence tomography. Opt Express. 2003;11:2183-9.

[29] de Melo LS, de Araujo RE, Freitas AZ, Zezell D, Vieira ND, Girkin J, et al. Evaluation of enamel dental restoration interface by optical coherence tomography. J Biomed Opt. 2005;10:064027.

[30] Sinescu C, Negrutiu ML, Todea C, Balabuc C, Filip L, Rominu R, et al. Quality assessment of dental treatments using en-face optical coherence tomography. J Biomed Opt. 2008;13:054065.

[31] Ozawa N, Sumi Y, Shimozato K, Chong C, Kurabayashi T. In vivo imaging of human labial glands using advanced optical coherence tomography. Oral Surg Oral Med Oral Pathol Oral Radiol Endod. 2009;108:425-9.

[32] Girish V, Vijayalakshmi A. Affordable image analysis using NIH Image/ImageJ. Indian J Cancer. 2004;41:47.

[33] Ridler T, Calvard S. Picture thresholding using an iterative selection method. IEEE Transactions on Systems, Man and Cybernetics. 1978:630-2.

[34] Sadr A, Shimada Y, Mayoral JR, Hariri I, Bakhsh TA, Sumi S, et al. Swept source optical coherence tomography for quantitative and

qualitative assessment of dental composite restorations. Lasers in Dentistry XVII. San Francisco, California, USA: Proc. SPIE; 2011.

[35] Makishi P, Shimada Y, Sadr A, Tagami J, Sumi Y. Non-destructive 3D imaging of composite restorations using optical coherence tomography: Marginal adaptation of self-etch adhesives. J Dent. 2011.

[36] Meng Z, Yao XS, Yao H, Liang Y, Liu T, Li Y, et al. Measurement of the refractive index of human teeth by optical coherence tomography. J Biomed Opt. 2009;14:034010.

[37] Dunkers JP, Parnas RS, Zimba CG, Peterson RC, Flynn KM, Fujimoto JG, et al. Optical coherence tomography of glass reinforced polymer composites. Composites Part a-Applied Science and Manufacturing. 1999;30:139-45.

[38] Ikeda I, Otsuki M, Sadr A, Nomura T, Kishikawa R, Tagami J. Effect of filler content of flowable composites on resin-cavity interface. Dent Mater J. 2009;28:679-85.

[39] Pioch T, Stotz S, Staehle HJ, Duschner H. Applications of confocal laser scanning microscopy to dental bonding. Adv Dent Res. 1997;11:453-61.

[40] Zeiger DN, Sun J, Schumacher GE, Lin-Gibson S. Evaluation of dental composite shrinkage and leakage in extracted teeth using X-ray microcomputed tomography. Dent Mater. 2009;25:1213-20.

[41] Sadr A, Shimada Y, Tagami J. Effects of solvent drying time on micro-shear bond strength and mechanical properties of two self-etching adhesive systems. Dent Mater. 2007;23:1114-9.

[42] Munksgaard EC, Hansen EK, Kato H. Wall-to-wall polymerization contraction of composite resins versus filler content. Scand J Dent Res. 1987;95:526-31.

[43] Aw TC, Nicholls JI. Polymerization shrinkage of densely-filled resin composites. Oper Dent. 2001;26:498-504.

[44] Chen HY, Manhart J, Hickel R, Kunzelmann KH. Polymerization contraction stress in light-cured packable composite resins. Dent Mater. 2001;17:253-9.

[45] Kishikawa R, Koiwa A, Chikawa H, Cho E, Inai N, Tagami J. Effect of cavity form on adhesion to cavity floor. Am J Dent. 2005;18:311-4.

[46] Kwon YH, Jeon GH, Jang CM, Seol HJ, Kim HI. Evaluation of polymerization of light-curing hybrid composite resins. J Biomed Mater Res B Appl Biomater. 2006;76:106-13.

[47] Ruttermann S, Kruger S, Raab WH, Janda R. Polymerization shrinkage and hygroscopic expansion of contemporary posterior resin-based filling materials--a comparative study. J Dent. 2007;35:806-13.

[48] Sadr A, Mayoral Molina J, Shimada Y, Bakhsh TA, Cho E, Tagami J. Real-time tomographic monitoring of composite restoration placement using SS-OCT. J Dent Res. 2010;89:1501.

[49] Tagami J, Nikaido T, Nakajima M, Shimada Y. Relationship between bond strength tests and other in vitro phenomena. Dent Mater. 2010;26:e94-9.

[50] Cho E, Sadr A, Inai N, Tagami J. Evaluation of resin composite polymerization by three dimensional micro-CT imaging and nanoindentation. Dental Materials. 2011;27:1070-8.

[51] Natsume Y, Nakashima S, Sadr A, Shimada Y, Tagami J, Sumi Y. Estimation of lesion progress in artificial root caries by swept source optical coherence tomography in comparison to transverse microradiography. Journal of Biomedical Optics. 2011;16.

[52] He Z, Shimada Y, Sadr A, Ikeda M, Tagami J. The Effects of Cavity Size and Filling Method on the Bonding to Class I Cavities. Journal of Adhesive Dentistry. 2008;10:447-53.

[53] Rees JS, Jacobsen PH. The polymerization shrinkage of composite resins. Dent Mater. 1989;5:41-4.

[54] de Gee AF, Feilzer AJ, Davidson CL. True linear polymerization shrinkage of unfilled resins and composites determined with a linometer. Dent Mater. 1993;9:11-4.

[55] Lai JH, Johnson AE. Measuring polymerization shrinkage of photo-activated restorative materials by a water-filled dilatometer. Dent Mater. 1993;9:139-43.

[56] Lovell L, Stansbury J, Syrpes D, Bowman C. Effects of composition and reactivity on the reaction kinetics of dimethacrylate dimethacrylate copolymerizations. Macromolecules. 1999:3913-21.

[57] Sideridou I, Tserki V, Papanastasiou G. Effect of chemical structure on degree of conversion in light-cured dimethacrylate-based dental resins. Biomaterials. 2002:1819-29.

[58] Carvalho RM, Pereira JC, Yoshiyama M, Pashley DH. A review of polymerization contraction: the influence of stress development versus stress relief. Oper Dent. 1996;21:17-24.

[59] Mjör IA, Toffenetti F. Secondary caries: a literature review with case reports. Quintessence Int. 2000;31:165-79.

[60] Watts DC, Amer O, Combe EC. Characteristics of visible-light-activated composite systems. Br Dent J. 1984;156:209-15.

[61] Lutz E, Krejci I, Oldenburg TR. Elimination of polymerization stresses at the margins of posterior composite resin restorations: a new restorative technique. Quintessence Int. 1986;17:777-84.

[62] Winkler MM, Katona TR, Paydar NH. Finite element stress analysis of three filling techniques for class V light-cured composite restorations. J Dent Res. 1996;75:1477-83.

[63] Yoshikawa T, Sano H, Burrow MF, Tagami J, Pashley DH. Effects of dentin depth and cavity configuration on bond strength. J Dent Res. 1999;78:898-905.

[64] Chikawa H, Inai N, Cho E, Kishikawa R, Otsuki M, Foxton RM, et al. Effect of incremental filling technique on adhesion of light-cured resin composite to cavity floor. Dent Mater J. 2006;25:503-8.

[65] Nikolaenko SA, Lohbauer U, Roggendorf M, Petschelt A, Dasch W, Frankenberger R. Influence of c-factor and layering technique on microtensile bond strength to dentin. Dent Mater. 2004;20:579-85.

[66] Cho E, Chikawa H, Kishikawa R, Inai N, Otsuki M, Foxton RM, et al. Influence of elasticity on gap formation in a lining technique with flowable composite. Dent Mater J. 2006;25:538-44.

[67] Sano H, Shono T, Sonoda H, Takatsu T, Ciucchi B, Carvalho R, et al. Relationship between surface area for adhesion and tensile bond strength--evaluation of a micro-tensile bond test. Dent Mater. 1994;10:236-40.

[68] Shono Y, Ogawa T, Terashita M, Carvalho RM, Pashley EL, Pashley DH. Regional measurement of resin-dentin bonding as an array. J Dent Res. 1999;78:699-705.

[69] Yoshiyama M, Carvalho RM, Sano H, Horner JA, Brewer PD, Pashley DH. Regional bond strengths of resins to human root dentine. J Dent. 1996;24:435-42.

[70] Prati C, Simpson M, Mitchem J, Tao L, Pashley DH. Relationship between bond strength and microleakage measured in the same Class I restorations. Dental Materials. 1992;8:37-41.

[71] Shirai K, De Munck J, Yoshida Y, Inoue S, Lambrechts P, Suzuki K, et al. Effect of cavity configuration and aging on the bonding effectiveness of six adhesives to dentin. Dental Materials. 2005;21:110-24.

[72] Dennison JB, Sarrett DC. Prediction and diagnosis of clinical outcomes affecting restoration margins. J Oral Rehabil. 2012;39:301-18.

[73] Ishibashi K, Ozawa N, Tagami J, Sumi Y. Swept-source optical coherence tomography as a new tool to evaluate defects of resin-based composite restorations. J Dent. 2011;39:543-8.

[74] Jones RS, Staninec M, Fried D. Imaging artificial caries under composite sealants and restorations. J Biomed Opt. 2004;9:1297-304.

[75] Monteiro GQ, Montes MA, Gomes AS, Mota CC, Campello SL, Freitas AZ. Marginal analysis of resin composite restorative systems using optical coherence tomography. Dent Mater. 2011;27:e213-23.

[76] Heintze SD. Systematic reviews: I. The correlation between laboratory tests on marginal quality and bond strength. II. The correlation between marginal quality and clinical outcome. J Adhes Dent. 2007;9 Suppl 1:77-106.

[77] Cenci M, Demarco F, de Carvalho R. Class II composite resin restorations with two polymerization techniques: relationship between microtensile bond strength and marginal leakage. Journal of dentistry. 2005;33:603-10.

[78] Guzman-Ruiz S, Armstrong SR, Cobb DS, Vargas MA. Association between microtensile bond strength and leakage in the indirect resin composite/dentin adhesively bonded joint. Journal of dentistry. 2001;29:145-53.

[79] Hariri I, Sadr A, Shimada Y, Tagami J, Sumi Y. Effects of structural orientation of enamel and dentine on light attenuation and local refractive index: An optical coherence tomography study. J Dent. 2012;40:387-96.

[80] Yahagi C, Takagaki T, Sadr A, Ikeda M, Nikaido T, Tagami J. Effect of lining with a flowable composite on internal adaptation of direct

composite restorations using all-in-one adhesive systems. Dent Mater J. 2012;31:481-8.

[81] Ilie N, Kunzelmann KH, Hickel R. Evaluation of micro-tensile bond strengths of composite materials in comparison to their polymerization shrinkage. Dent Mater. 2006;22:593-601.

[82] Nayif MM, Nakajima M, Foxton RM, Tagami J. Bond strength and ultimate tensile strength of resin composite filled into dentine cavity; effect of bulk and incremental filling technique. J Dent. 2008;36:228-34.

[83] Sanares AM, Itthagarun A, King NM, Tay FR, Pashley DH. Adverse surface interactions between one-bottle light-cured adhesives and chemical-cured composites. Dent Mater. 2001;17:542-56.

[84] Itoh S, Nakajima M, Hosaka K, Okuma M, Takahashi M, Shinoda Y, et al. Dentin bond durability and water sorption/solubility of one-step self-etch adhesives. Dent Mater J. 2010;29:623-30.

BIOGRAPHY

BIOGRAPHY

Turki A. BAKHSH,   BDS,

Date of Birth: 20th Oct 1981

M. Status: Married

Nationality: Saudi

Turki A. Bakhsh,   BDS

Cariology and Operative Dentistry
Oral Restitution Department
Tokyo Medical and Dental University
Bunkyo-ku, Yushima 1-5-45
Tokyo 113-5849, Japan
Tel: +81-3-5803-5483
Fax: +81-3-5803-0195
E-mail: taabakhsh@kau.edu.sa

EDUCATION

- 1999~2005   (BDS) Bachelor in Dental Medicine and Surgery in King Abdulaziz University (KAU), Jeddah, SAUDI ARABIA (SA)

PROFESSIONAL EXPERIENCE

- 2011~2013   Cariology and Operative Dentistry, TMDU hospital, JAPAN
- 2008~2009   Operative Dentistry, KAU hospital, Jeddah, SA
- 2006~2008   General Dentist, Ministry of Health, Makkah, SA
- 2005~2006   Internship, KAU hospital, Jeddah, SA

POSITIONS AND ACADEMIC EXPERIENCE

- May~Sep 2013   President of Saudi Arabian Students' Association in JAPAN.

- Jun 2013   Organizing Committee "OCT in Dentistry Symposium" TMDU

- 2011~ Present   Traveling lecturer, Optical Society of America (OSA)

- 2011~2013   President of TMDU Student Chapter of OSA

- 2010~2013   Teaching Assistant, Cariology and Operative Dentistry,   Faculty of Dentistry, TMDU

- 2010~2013   Advanced. I. Super Student in Global Center of Excellence (AISS-GCOE) program entitled "International research center for Molecular Science in Tooth and Bone Diseases" TMDU

- 2010~2011   Secretory of TMDU Student Chapter of OSA

- 2008~2013 Demonstrator and Clinical Instructor, Operative Dentistry, Faculty of Dentistry, KAU

- 2006~2007   Member of the Organizing Committee "Saudi Dental Society"

PART-TIME PROFESSIONAL PRACTICE

- Jul~Sep 2009   King Abdulaziz Medical City, Alwaha Health Center, Jeddah, SA.

- Jun~Sep 2008   King Khaled National Guard Primary Health Care Center, Makkah, SA.

PROFESSIONAL QUALIFICATION

- Oct 2012   **American Academy of Facial Esthetics Certificate** in "Dermal Fillers Training for Health Professionals - Hands-On Training" Salt Lake City, USA

- Oct 2012 **American Academy of Facial Esthetics Certificate** in "Botulinum Toxin Training for Health Professionals - Hands-On Training" Salt Lake City, USA

- 2011 **Basic Life Support (BLS) Certificate** "Tokyo Medical and Dental University", JAPAN

- 2005 **Saudi Council for Health Specialties License**

- 2004 **Basic Life Support (BLS) Certificate** "Saudi Heart Association"

RESEARCH INTEREST

1. Advanced Bio-Medical imaging systems.
2. 3D Image analysis
3. Nano-technology in the restorative dental sciences
4. Lasers in Dentistry
5. Mechanism of dentin bonding
6. Adhesion of biomaterials to dental tissues
7. Advanced mechanical characterization of tooth-biomaterial bonding strength
8. Caries research
9. Physic-chemical and manipulative properties of restorative materials
10. Durability of restorative materials

11. Improvement of various esthetic restorative techniques for direct and indirect restorations

HONORS

- **Best Poster Award** in the 5th TMDU International Summer Program (ISP 2013). TMDU, JAPAN, 28th Aug 2013

- **Excellence Research Award** in the Graduation Ceremony of the First Batch of the Saudi Students' in Japan organized by Ministry of Higher Education (MOHE) - Saudi Cultural attaché Office. JAPAN, Mar 2013

- **Kobyashi Excellence Research Achievement Award** (TMDU) JAPAN, 8th Mar 2013

- **Princess Lulua Al-Faisal award** for the outstanding research achievement (Japanese-Saudi parliamentary Friendship society with Royal Embassy of Saudi Arabia in Japan). JAPAN, 7th Feb 2012

CONFERENCE PRESENTATION

1. **BAKHSH TA,** SADR A, SHIMADA Y, MANDURAH MM, ALSAYED EZ, KHUNKAR SJ, TAGAMI J, SUMI Y. OCT Assessment of the Adaptation of Polymeric Dental Restorations in Human

Teeth. The 5th TMDU International Summer Program (ISP 2013), TMDU, Tokyo, **JAPAN**. Poster Presentation. Aug 2013

2.   **BAKHSH TA,** SADR A, SHIMADA Y, MANDURAH MM, ALSAYED EZ, KHUNKAR SJ, TAGAMI J, SUMI Y. Relationship between OCT image, Microscopic Gap and Bond Strength of Composites. The 1st International Symposium and Mini-Exhibition for Optical Coherence Tomography in Dentistry Symposium, TMDU, Tokyo, **JAPAN**. Oral Presentation. Jun 2013

3.   **BAKHSH TA,** SADR A, SHIMADA Y, MANDURAH M, ALSAYED E.Z, TAGAMI J, SUMI Y. Non-destructive Evaluation of Internal Cavity Adaptation in Class-II resin Composite. The 91st General session and exhibition for **IADR, 42nd AADR and 37th CADR**. Seattle General Session and Exhibition, **USA**. Oral presentation. Mar 2013

4.   **BAKHSH TA,** SADR A, SHIMADA Y, MANDURAH M, TAGAMI J, SUMI Y. Optical Evaluation of Composite Adaptation in Class-II Restoration. Molecular science in oral systematic medicine seminar.   GCOE, TMDU, Tokyo, **JAPAN**. Poster Presentation. Feb 2013

5.   **BAKHSH TA,** SADR A, SHIMADA Y, MANDURAH M, TAGAMI J, SUMI Y. Optical Evaluation of Composite Adaptation in Class-II Restoration. International Student Research Day. **Global-COE**, TMDU, Tokyo, **JAPAN**. Poster Presentation. Nov 2012

6.   **BAKHSH TA,** SADR A, SHIMADA Y, TAGAMI J, SUMI Y. Optical Comparison between One-step and Two-step self-etch adhesives in Restored Class-I Cavities. Student Leadership

Conference **OSA-FiO**, Rochester, **USA**. Poster presentation. Oct 2012

7.   **BAKHSH TA**, SADR A, SHIMADA Y, TURKISTANI A, TAGAMI J. SUMI Y. Optical Evaluation of Composite Adaption in Class-II Cavity Restoration using SS-OCT. The 136th **JSCD**, Okinawa, **JAPAN**. Oral presentation. Jun 2012

8.   **BAKHSH TA**, SADR A, SHIMADA Y, MANDURH M, TAKAGAKI T, TAGAMI J. Ultrastructural Assessment of Tooth-Resin Interface using FIB-TEM Technology. The **90th IADR** General Session and Exhibition, Foz do Iguaçu, **BRAZIL**. Oral presentation. Jun 2012

9.   **BAKHSH TA**, SADR A, SHIMADA Y, TAGAMI J, SUMI Y. Non-invasive Evaluation of Composite Failure using SS-OCT. The 6th Global COE International Symposium, Tokyo, **JAPAN**. Poster presentation. Jan 2012

10.   **BAKHSH TA**, SADR A, SHIMADA Y, KHUNKAR S, TAGAMI J, SUMI Y. Relationship between Non-destructive OCT Evaluation of Resins Composites and Bond Strength in a Cavity. Lasers in Dentistry XVIII. BiOS **SPIE** Photonic West. San Francisco, **USA**. Oral presentation. Jan 2012

11.   **BAKHSH TA**, SADR A, SHIMADA Y, SUMI Y, TAGAMI J. Composite Failure Assessment in Different Filling Techniques using SS-OCT. 59th **JADR**, Hiroshima, **JAPAN**. Poster presentation, Oct 2011

12.   SADR A, SHIMADA Y, MAYORAL JR, HARIRI I, **BAKHSH TA**, SUMI Y, et al. Swept source optical coherence tomography

131

for quantitative and qualitative assessment of dental composite restorations. Lasers in Dentistry XVII. Proc. BiOS **SPIE** Photonics West. San Francisco, California, **USA**. Jan 2011

13.   SADR A, HARIRI I, NAZARI A., **BAKHSH TA**, SHIMADA Y, NAKASHIMA S, SUMI Y, and TAGAMI J. Demineralization Affects Refractive Indices of Human Enamel and Dentin, **88th IADR**, Barcelona, **SPAIN**. Oral presentation. July 2010

14.   **BAKHSH TA**, SADR A, SHIMADA Y, MAKISHI P, MAYORAL JR, SUMI Y, TAGAMI J. Comparison between SS-OCT & CLSM in assessment of restoration defects. The **88th IADR** General Session and Exhibition, Barcelona, **SPAIN**. Oral presentation. July 2010

15.   Review on Local anesthetics failure in Endodontic. Faculty of Dentistry, KAU, Jeddah, **S.A.** Oral Presentation. 2006

16.   Literature review on the Uses of Micro C.T. in Endodontic. King Fahad Armed Forces Hospital, Jeddah, **SA**. Oral Presentation. 2006

CONFERENCES, SEMINARS & WORKSHOPS

- **Course & Workshop** in "Application of Soft tissue Lasers - Advanced Hands-On Training – Part II" Yoshida Dental. Tokyo, JAPAN. 2013

- **Certificate of Attendance** "The 91st General session and exhibition for **IADR, 42nd AADR and 37th CADR.** Seattle General Session and Exhibition, **USA**. Mar 2013

- **Certificate of Attendance** "General Meeting of the Japan section, International College of Dentists **(ICD)"** May 2012

- **Course and Hands-On Training** in "CAD-CAM & GIC Cement's Applications" GC Dental Corp. Tokyo, JAPAN. 2012

- **Course & Workshop** in "Application of Soft Tissue Laser - Advanced Hands-On Training – Part I" Yoshida Dental. Tokyo, JAPAN. 2012

- **Certificate of Attendance** "The **90th IADR** General Session and Exhibition" Foz do Iguaçu, **BRAZIL**. Jun 2012

- **Certificate of Attendance** "The **89th IADR** General Session and Exhibition" San Diego, **USA**. Mar 2011

- **Seminar & Workshop** in "Novelty of 3D self-reinforcing (SR) monomer" Tokuyama Dental. Tsukuba, JAPAN. 2011

- **Certificate of Attendance** "The **88th IADR** General Session and Exhibition" Barcelona, **SPAIN**. July 2010

- **Certificate of Attendance "I TMDU-UIC Restorative Dentistry Joint Symposium"** Sant Caugat del Vallés, **SPAIN**. July 2010

- **Course & Workshop** in "Evidence Based Dentistry". Jeddah, S.A. 2008

- **Certificate of Attendance** "2nd International King Abdulaziz University & 19th Saudi Dental Society Conference for Dental Research and Technology Conference" Jeddah, S.A. 2008

- **Course & Workshop** "Advanced XIVE implants system" DENTSPLY FRIADENT. Jeddah, S.A. 2007l

- **Course & Workshop** in "Management of medically compromised patient". Jeddah, S.A. 2004

- **Certificate of Attendance** "UAE International Dental Conference and Arab Dental exhibition" ADEEC DUBAI" UAE. 2004

PROFESSIONAL MEMBERSHIPS

- Member of International Association of Dental Research (IADR)
- Member of International Association of Dental Research, Japanese division (JADR)

- Member of International Association of Dental Research, Saudi Arabian division

- Super-student Member of Global Center Of excellence (AISS-GCOE)

- Member of Academy of Operative Dentistry (AOD)

- Member of American Academy of Cosmetic Dentistry (AACD)

- Member of the Optical Society of America (OSA)

- Member of SPIE (Society of Photo-Optical Instrumentation Engineers)

- Member of International Society of Infectious Diseases (ISID)

- Past-Member of Saudi Dental Society (SDS)

PUBLICATIOIONS

1. Mandurah MM, Sadr A, Shimada Y, Kitasako Y, Nakashima S, **Bakhsh TA**, Tagami J, Yasunori S. Monitoring Remineralization of Enamel Subsurface Lesions by Optical Coherence Tomography. J Biomed Opt. Mar 2013 (doi:10.1117/1.JBO.18.4.046006).

2. **Bakhsh TA**, Sadr A, Shimada Y, Mandurah M, Hariri I, Alsayed E, Tagami J, Sumi Y. Concurrent Evaluation of Composite Internal Adaptation and Bond Strength in a Class-I Cavity. J Dent. Oct 2012. Doi: 10.1016/j.jdent.2012.10.003.

3. **Bakhsh TA**, Sadr A, Shimada Y, Khunkar S, Tagami J, Sumi Y. Relationship between Non-destructive OCT Evaluation of Resins Composites and Bond Strength in a Cavity. Proc. SPIE 2012;8208:820809.

4. Sadr A, Shimada Y, Mayoral JR, Hariri I, **Bakhsh TA**, Sumi Y, et al. Swept source optical coherence tomography for quantitative and qualitative assessment of dental composite restorations. Proc. SPIE 2011;7884:78840C.

5. **Bakhsh TA**, Sadr A, Shimada Y, Tagami J, Sumi Y. Non-invasive quantification of resin-dentin interfacial gaps using optical coherence tomography: Validation against confocal microscopy. Dent Mater 2011;27:915-25.

<u>SPECIAL SKILLS & LANGUAGE SKILLS</u>

- Professional - computers, photography and cooking.
- Activities - camping, hiking, traveling, reading, playing volleyball, bowling and social gatherings.
- Fluent - Arabic & English languages (Reading, Writing, Listening & Speaking).
- Very Good - Hindi and Acceptable in Japanese language (Listening & Speaking).

2013